UNIVERSIDAD DE GUANAJUATO

CAMPUS GUANAJUATO/DIVISIÓN DE INGENIERÍAS

"ASSESSING THE IMPACT OF CLIMATE CHANGE ON WATER RESOURCES WITH SWAT MODEL FOR A SEMI-ARID REGION OF GUANAJUATO STATE, CENTRAL MEXICO"

TESIS

Que para obtener el Título de

CIENCIAS DEL AGUA

Presenta:

CHAO DENG

Directores:

DRA. YANMEI LI

DR. JESÚS HORACIO HERNÁNDEZ ANGUIANO

Guanajuato, Gto. Agosto de 2017

Abstract

A Soil and Water Assessment Tool (SWAT) model was developed for the Independence Basin, a watershed of around6,992.00 km^2 with significant seasonal climate in the semi-arid highland of central Mexico, Guanajuato state. This area is dominated by agricultural land cover (43.32%) and followed by pasture (25.70%). This study aims to evaluate the historical variation of water resources and the impacts of future climate change on the hydrologic regime of the Independence Basin. Thus, the Independence Basin was divided into 36 sub-basins by ArcSWAT (Version 2012) and calibrated with 2 gauging stations and 2 reservoirs data sets with the aid of the SUFI-2 algorithm assembled in SWAT-CUP. Hydrological responses to future climate change have been analyzed under conditions of RCP 4.5 emission scenario and RCP 8.5 emission scenario generated by 7 General Circulation Models (GCMs) for the mid-century period (2030-2059) and for the end of this century (2070-2099), respectively.

In modeling the stream flow, results from good to very-good fit level with R^2 (0.66~0.89) and Nash–Sutcliffe efficiency (NSE) (0.65~0.88) have been obtained for both the calibration and the validation periods, while the PBIAS was not as good as the former indicators but nevertheless very-good to satisfactory results were obtained. Five of those parameters: CN2, SOL_K, SOL_AWC, GWQMN and SOL_Z are sensitive in descending order in the Independence Basin model, indicating that the groundwater system plays an important role in the hydrologic regime. The historical water budget analysis of a 40-years period of 1970-2009 showed that the annual precipitation was about 495.10 mm, while PET, ET, deep aquifer recharge and surface runoff were 1670.00 mm, 471.30 mm, 39.08 mm and 33.38 mm, respectively. The estimated groundwater extraction was lower than the real case, indicating that the drawdown of aquifers has been worsened in recent years.

According to the projections of 7 GCMs, the Independence Basin may experience higher precipitation and temperature under all the emission scenarios for both periods compared to the baseline condition (1970-1999). For future climate change, PET was estimated to increase continuously from 6.7%-8.3% in the period of 2030-2059 to 9.9% - 17.1% in the period of 2070-2099, while ET increases at lower rates. Both mean annual surface runoff and deep aquifer recharge were simulated to increase more rapidly under the condition of scenario RCP 8.5 than that of RCP 4.5. Under the emission scenario of RCP 4.5, the increasing rates of surface water recharge and deep aquifer recharge will slow down at the end of this century when compared to the mid-century rates. As induced by the increasing PET, groundwater extraction would be augmented gradually under current management status. It was estimated an increasing demand of 8.4% and 24.2% of groundwater exploitation for agricultural irrigation at the end of this century under emission scenarios of RCP 4.5 and RCP 8.5, respectively. It also has been predicted that no chance of aquifer recovering would happen in the future under condition of climate change. Meanwhile, the drawdown rate of water table in the Independence Basin would remain the same as in the present in the mid-century, and then it would accelerate at the end of this century.

Understanding the impacts of potential climate changes is important for sustainable water resource management in the Independence Basin with intensive groundwater pumping activities. The findings of this study can be useful for decision makers and planners to design adaptive measures to climate changes. This study also has valuable implications for watershed modeling research for semi-arid regions.

Resumen

Se desarrolló un modelo hidrológico (SWAT: Soil and Water Assessment Tool) para la Cuenca de la Independencia, una cuenca de alrededor de 6,992.00 km^2 con clima estacional significativo en el altiplano semiárido del centro de México, estado de Guanajuato. Esta área está dominada por la cubierta de la tierra agrícola (43.32%) y seguida por la pastura (25.70%). Este estudio tiene como objetivo evaluar la variación histórica de los recursos hídricos y los impactos del cambio climático futuro en el régimen hidrológico de la Cuenca de la Independencia. Así, la Cuenca de la Independencia fue dividida en 36 subcuencas por ArcSWAT (Versión 2012) y calibrada con 2 estaciones de medición y 2 archivos de depósitos con la ayuda del algoritmo SUFI-2 montado en SWAT-CUP individualmente. Las respuestas hidrológicas al cambio climático futuro se han analizado bajo las condiciones del escenario de emisiones del RCP 4.5 y del escenario de emisiones del RCP 8.5 por 7 modelos de circulación general (MCG) para el período de mediados de siglo (2030-2059) y al final de este siglo (2070- 2099), respectivamente.

En el modelado del flujo de la corriente, se han obtenido resultados buenos a muy buenos con R^2 (0.66 ~ 0.89) y NSE (0.65 ~ 0.88) durante el período de calibración y la duración de validación, mientras que el PBIAS fue peor A resultados muy buenos. CN2, SOL_K, SOL_AWC, GWQMN y SOL_Z son 5 parámetros sensibles en orden descendente en la Cuenca de la Independencia, lo que indica que el sistema de aguas subterráneas juega un papel importante en el régimen hidrológico. El análisis histórico del presupuesto de agua de un período de 40 años de 1970-2009 mostró que la precipitación anual fue de unos 495.10 mm, mientras que PET, ET, recarga profunda del acuífero y escurrimiento superficial fueron 1,670.00 mm, 471.30 mm, 39.08 mm y 33.38 mm,

respectivamente. La extracción estimada de agua subterránea fue inferior a la del caso real, lo que indica que el inconveniente de los acuíferos se ha agravado en los últimos años.

De acuerdo con las proyecciones de 7 MCG, la Cuenca de la Independencia puede experimentar mayores precipitaciones y temperaturas bajo todos los escenarios de emisión para ambos períodos en comparación con la condición de base (1970-1999). Para el cambio climático futuro, se estimó que el PET aumentaría continuamente de 6.70% -8.30% en el período 2030-2058 a 9.90% -17.10% en el período de 2070-2099, mientras que el ET aumentaría a tasas más bajas. Se simularon tanto la escorrentía superficial anual media como la recarga profunda del acuífero para aumentar más rápidamente bajo la condición del escenario RCP 8.5 que la de RCP 4.5. Bajo el escenario de emisiones del RCP 4.5, las tasas crecientes de recarga superficial y de recarga profunda del acuífero se desacelerarán a fines de este siglo, en comparación con la mitad del siglo. Como inducido por el aumento de PET, la extracción de agua subterránea se exageraría gradualmente bajo el estado de manejo actual. Se estimó una demanda creciente de 8.40% y 24.20% de explotación de aguas subterráneas para riego agrícola a fines de este siglo bajo escenarios de emisiones de RCP 4.5 y RCP 8.5, respectivamente. Se ha predicho que ninguna posibilidad de recuperación del acuífero ocurriría en el futuro bajo la condición del cambio climático. Mientras tanto, la bajada de la capa freática en la Cuenca de la Independencia seguiría siendo la tasa actual a mediados de siglo, pero para acelerar a finales de este siglo.

La comprensión de los impactos de los posibles cambios climáticos es importante para el manejo sostenible de los recursos hídricos en la Cuenca de la Independencia, con actividades intensivas de bombeo de aguas subterráneas. Los resultados de este estudio pueden ser útiles para que los tomadores de decisiones y los planificadores diseñen medidas adaptativas a los cambios climáticos. Este estudio también tiene implicaciones valiosas para la investigación del modelado de cuencas hidrográficas para regiones semiáridas.

Contents

Chapter 1 Introduction

Water is the basis of the life of the universe with different forms existing in nature and participating in physical, biological and chemical processes. The role of water acts as an important carrier of material and energy. The total amount of water on Earth is about 1.4 billion cubic meters while the fresh water only occupies 2.50%, i.e. 35.00 Mm^3 (USGS). However, groundwater constitutes about 97.00% of anthropic potential available freshwater resources with a limited portion of 30.00% of the freshwater resources. The characteristics of generally high-quality and almost ubiquitous distribution promote the groundwater as the source of 35.00% freshwater withdrawals worldwide, supplying an estimated 36.00%, 42.00% and 27.00% of the water consumed for domestic, agricultural and industrial purposes, respectively (Döll et al., 2012). In Mexico, the spatial distribution of water contrasts with the distributions of economic activity and population: low water availability group covering 40.00% of the population and generating 51.00% of the GDP while medium water availability group and high water availability group consisting of 50.00%, 10.00% of population and accounting 42.00%, 7.00% of the GDP, respectively (Lopez-Morales and Duchin, 2015). Groundwater exploitation accounts for 37.50% of total freshwater withdrawals and the water stress is intimately linked to agriculture in Mexico, which consumes 77.00% of withdrawals (UN-Water, 2013).

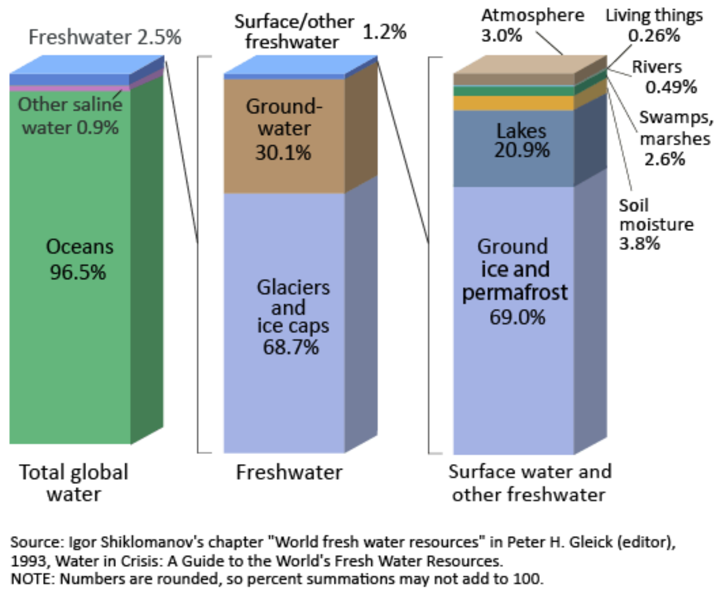

Fig. 1-1 Distribution of water resources (Gleick, 1993)

1.1 Water consumption in Guanajuato

Guanajuato, situated in the upper part of the Lerma-Chapala river basin, lies in the Bajío region in the north of the central mexican highlands with a semi-arid climate of a marked rainfall season between May and October, mostly with afternoon thunderstorms. Annual precipitation varies from 400-800 mm with an average value of about 650 mm over its covering area of 30,768 km². The region not only has seasonal rainfalls but they also vary spatially, with the more southern areas receiving slightly more precipitation than the central locations (Endfield et al., 2004). This state is divided into 20 individual aquifers under the definition of CONAGUA as shown in Fig. 1-2. The unevenly groundwater distribution pattern (CEAG, 2014) shows that water depth is higher in the northern part than in the southern areas, such as Silao and Romita.

Fig. 1-2 The 20 aquifers in Guanajuato under the definition of CONAGUA

The demand of water for urban use in Guanajuato comes fundamentally from the population growth in large cities (over one hundred thousand inhabitants) and medium ones (twenty thousand to one hundred thousand inhabitants). The statistic annual average growth rate of the urban population was 1.67% during the period 2000-2005, and the urbanized population would increase by 76.00% by the end of 2015 in Guanajuato state (Guzman-Soria et al., 2013).

Water consumption, maintaining a positive correlation with the population growth in both large cities and medium cities during the period of 2000 to 2011, increased by 17.20 Mm^3 in 2011 when compared to the recorded 243.00 Mm^3 in 2000. Simultaneously, various industrial parks consumed 9.40 Mm^3 more in 2011 than in 2000.

Statistically, the annual groundwater extraction in the year 2014 was 3,934.00 Mm^3 while the total recharge volume was estimated to be 2,795.00 Mm^3, resulting in a deficit of 1,139.00 Mm^3 (CEAG, 2014). In the same year, 76.00% of the active exploitation points and 84.00% of the extracted groundwater was used for agricultural irrigation. Based on the econometric assessment work of Guzman-Soria et al. (2013), the increase of the water prices has reduced urban and industrial water consumption. Thus, Guanajuato state suffers from water shortages that will restrict a sustainable development in a long term.

1.2 Water management state

1.2.1 Law framework

- National Water Law

"Water is owned by the Nation", written in Article 27 of the Constitution of Mexico, gives the ownership of water resources to the nation within its national boundary (Cortés and Maravilla, 2011). In 1992, the National Water Law (NWL) was promulgated for integrated water management with all stakeholders, to achieve sustainable development and good service of water resources. The amended version in 2004, more extensive and explicit than the older one, aims to restructure CONAGUA key functions through the decentralization process: strengthening the administration of subnational entities. The articles relating to groundwater management in NWL is shown in the followings:

Article LIV. "Environmental Use" or "Use for ecological conservation": The minimum volume flow or necessary in receiving bodies, including streams and reservoirs of various kinds, or the minimum flow of natural discharge of an aquifer, that has to be kept in order to protect the environmental conditions and the ecological balance of the system.

Article LXIII. "Regulated area": Specific areas of aquifers, watersheds or hydrological regions, which require a specific water management to ensure hydrological sustainability because their natural deterioration, water unbalance, risks or damage to bodies of water or the environment, fragility of vital ecosystems, overexploitation, and as well for its reorganization and restoration.

Article LXV. "Closed zone": Specific areas of hydrological regions, watersheds or aquifers, in which it is not permitted additional water abstractions to those established legally, and the latter are controlled by specific regulations, by reasons of the deterioration of water sources in terms of quantity or quality, the adverse effects on the hydrological sustainability, or because the damage to surface or underground water bodies.

- Federal Executive

Article 6. Compete the Federal Executive

I. Regulate by watershed and aquifer monitoring the extraction and exploitation, use or utilization of national groundwater, including those that have been freely lit, and the surface, under the terms of Title V of this Law; and issue decrees for the establishment, modification or deletion of regulated areas in which require specific hydrological management to ensure the sustainability of vital ecosystems identified in aquifers, watersheds, hydrologic regions or areas compromised.

Article 7. Declared of public utility:

II. The protection, improvement, conservation and restoration of watersheds, aquifers, streams, vessels and other water tanks national ownership, catchment sources of supply, federal zones and natural or artificial infiltration of water to replenish aquifers according to the "Mexican Official Standards" and the diversion of water from a basin or hydrological region to another.

V. Restoring national hydrological balance, surface and subsurface waters, including limited extraction in regulated areas, closures, reserves and change in water use to be earmarked for domestic use and urban public, artificial recharge, and the provision of water to the soil and subsoil according to current regulations.

- Water Planning and Programming

III. Specific, sub-regional, state hydrological basins, aquifers, and which address sectoral shortage or water pollution, order management of watersheds and aquifers, or correct the overexploitation of surface and groundwater; these subroutines include the use of instruments to address conflicts overexploitation, use, development and conservation of water quantity and quality, the problem of concession allocation and transfer of rights to use water in general to operate, use, including reuse and control, preservation and restoration thereof; the development and updating of the inventory of national waters and their inherent public goods as well as the uses of water, including the Public Registry of Water Rights and infrastructure for exploitation and control.

VI. The classification of water bodies according to their intended use and the development of ***water balance*** in quantity and quality and watersheds, aquifers and hydrologic regions, according to the load capacity thereof.

Article 86. "The Water Authority" will be responsible in terms of Law:

Promote and, where appropriate, implement and operate the federal infrastructure, monitoring systems and services necessary for the preservation, conservation and improvement of water quality in watersheds and aquifers, according to the Mexican Official Standards respective and specific discharge conditions.

III. Develop comprehensive programs to protect water resources in watersheds and aquifers, considering the relationship between land use and the quantity and quality of water.

Article 91. The infiltration of wastewater to recharge aquifers, requires permission from "the Water Authority" and must comply with the Official Mexican Standards issued for such purpose.

- General Law of Ecological Balance and Environmental Protection

Article 88. For the sustainable use of water and aquatic ecosystems the following criteria are considered:

I. The State and society protection of aquatic ecosystems and balance of natural elements involved in the hydrological cycle;

II. To maintain the integrity and balance of natural elements involved in the hydrological cycle, you should consider the protection of soil and forest and jungle areas and maintaining basic flow of streams, and the ability to recharge aquifer.

III. All of them above.

1.2.2 Institutional framework

- CONAGUA

Mexico initiated the water reforms from the late 1980s onwards to an integrated water resource management, thus created a federal water agency, the Comisión Nacional de Agua (CONAGUA).

In the 1990s major efforts were made by federal government water agency (the CNA) to register and administer the groundwater abstraction and use rights system. However, the system has been eroded by lack of local operational resources and failure to mobilize user cooperation. Lack of consistent enforcement meant that those who decide not to follow the rules are usually not sanctioned, thus deterring the rest of the users from cooperating or complying with the regulation processes.

- **CEAG**

In 1991, the CEAG, short for Comisión Estatal del Agua en Guanajuato, was created as a decentralized public entity for the provision of potable water, sewage removal, and sanitation. Until late 1995, the main function of the CEAG was to coordinate and execute potable water and sewage programs in urban and rural areas. In its first 4 years, it had two directors. In May 1995, Vicente Fox named Vicente Guerrero, then President of the Council for System of Water and Sewage of Leon (SAPAL), as the new director of the CEAG, who implemented institutional changes that generated a broader focus for the organization. This permitted CEAG to tackle more effectively water problems of the state.

- COTAS

After the new Mexican Water Law was promulgated in December 1992, the CONAGUA promoted nationally the establishment of civil society organizations (*Consejo Técnicos de Aguas*, COTAS) to help address the challenge of groundwater resource management, especially in about 100 overdrafted aquifers. In 1997 the first COTAS started to work and the total 20 aquifers were covered in Guanajuato. Each individual COTAS is financially supported by Guanajuato State Government through a state trust fund and the governing board of a COTAS is constituted exclusively from groundwater users. The main objectives are set as: a) represent all water users in the region, b) participate in the regulations for the use, exploitation and use of water, to be convened by the water authorities, c) establish itself as liaison bodies, cooperation of users in coordination with the various authorities to solve problems and needs, d) to respect and ensure compliance with their constituents and associated legal and administrative arrangements for water, e) to cooperate with the competent authorities in the formulation, monitoring, evaluation and modification of plans and programs at state or regional water sector are implemented (Foster et al., 2004).

CEAG and COTAS are two most important administrative tools of groundwater resources here in Guanajuato. Currently, agriculture irrigation, industrial and public water supply consume huge volume of groundwater and potential pollution problems have been caused by the application of fertilizers, pesticides and the wastewater irrigation or recharge activities. Nevertheless, diagnostic studies of the degradation and depletion of groundwater resources are not sufficient yet, enough information about the water availability and water sources depletion is not given to the society. Fortunately, the COTAS are intended to be consensus-building spaces where integrated water management models and programs are to be implemented. With the help of training programs as well as the technical support from local universities and/or technical institutions, the staffs can be active and more proficient in monitoring the deep wells, providing more detailed information about the current status of groundwater resources in Guanajuato.

1.2.3 Plans and policy

- 2030 Water Agenda

In 2011, the CONAGUA issued the ambitious 2030 Water Agenda to control the non-point pollution, to balance the aquifer equilibrium and to apply the sate-of-the-art technology for warning and prevention systems at local, state and national level. In its balanced supply and demand for water section, the initiatives were written as follows:

Initiative 1: Giving a more relevant role to ONAGUA in aquifer management;

Initiative 3: Consolidating the governance functions and regional organization of the CONAGUA;

Initiative 4: Involving civil society associations of irrigation users (ACUs) and COTAS in driving for the saving of water and the technification of irrigation;

Initiative 5: Formulating regulations for the distribution of surface water by catchment and groundwater by aquifer.

- Environment and Natural Resources Sector Program

The Environment and Natural Resources Sector Program (PSMARN) takes environmental sustainability as its main reference framework, which fully relates it with the National Development Plan, which in turn refers to sustainability as one of the major lines that composes it.

Blue Agenda: Integrated Water Resources Management

- Promoting integrated catchment and aquifer management;

- Develop economic incentives and instruments that foster the preservation of ecosystems.

- National Water Plan (PNH 2014-2018)

Five guidelines are established in the PNH:

1. Water as an integrator of Mexicans.

2. Water as an element of social justice.

3. An informed and participatory society to promote a water-efficient culture.

4. Water as a promoter of sustainable development.

5. Mexico as a global example in water-related issues.

Objectives in the short, medium and long-term focus mainly on strengthening integrated and sustainable water management; increasing water security against droughts and floods; securing water for agricultural irrigation, energy, industry, tourism, and other economic and financial activities in a sustainable manner.

- The Guanajuato State Water Plan 2000-2025

To cope with the water problems, the Guanajuato government implemented an intense program — The Guanajuato State Water Plan 2000-2025 (Plan Estatal Hidráulico 2000–2025), for investing in efficient water-use technologies, as well as organizing and supporting water users. Within this whole program, the groundwater issue has been identified as fundamental since it represents a major obstacle to the state's future development and, in the near future, threatens the public supply (Sandoval, 2004).

- Energy subsidy

The electricity subsidies in agriculture, covering more than 60% of the electricity consumption in pumping irrigation (Muñoz Piña et al., 2006), is more than the investment to improve the irrigation infrastructures (OECD, 2013). The artificially lowering pumping prices induced by electricity subsidies has contributed to the less efficient use of groundwater and the severer overdraft of groundwater from aquifers. Additionally, the potential investment in more efficient irrigation technology is receded by the issued substantial electricity subsidies. Farmers who extract groundwater below a certain threshold are exempted from water resource charge. The synchronous support and subsidies in agreement and electricity can work against the water policy objectives, impacting detrimentally on groundwater management putting water security at risks.

Overall, many water governance gaps, not specific to the sectors of enforcement and compliance, accountability, uneven nature of decentralisation, informality, institutional quality and capacity of public administration and limited transparency, are faced by the government (shown in Table 1-1) (OECD, 2013).

Table 1-1 Multi-level governance gaps in Mexico's water sector

Type	Description and examples
Administrative gap	Mismatch between administrative and functional units (water bodies, municipalities, metropolitan areas, regions, states) and hydrological boundaries and imperatives.
Information gap	Asymmetry of information across stakeholders, limited standardisation, incomplete REDPA and metering system => public disclosure and harmonisation are key concerns.
Policy gap	Misaligned policies across water, energy, agricultural and territorial development policies Scattered planning tasks and capacity
Capacity gap	High turnover among water professionals, limited training programs for technical, administrative and management staff;
Funding gap	Very limited own-source revenues at sub-national level; Huge reliance on federal programs and CONAGUA resources.
Objective gap	Lack of continuity of public policy at local level because of limited political mandates (3-year term of Mayors); Contradictory motivations of RBO and RBC leadership
Accountability gap	Limited stakeholder engagement in WRM (farmers and indigenous communities) and WSS (users and consumers); Limited official mechanisms to channel' demands

1.3 Independence Basin

The Independence Basin, situated in the NNE of Guanajuato State in the Central Mexican Highland with coordinates from 100°15’ to 101°30’ W and from 20°50’ to 21°32’ N, respectively, covers a surface area of about 7,000.00 km^2 based on the digital model of elevation with elevation altitudes varying from 1,850.00 m to 2,850 m above the sea level. Several main municipalities such as San Miguel de Allende, Dolores Hidalgo, San Felipe, San Diego de la Unión, San Luis de la Paz, Dr. Mora and San José Iturbide. Río Laja is the main river in the basin and this sedimentary basin is surrounded by mountainous areas, including the Sierra del Cubo to the north, the Sierra de Santa Barbara to the northwest, the Sierra de Guanajuato to the west, the Palo Huerfano and La Joya volcanoes to the south, the Zamorano massif to the southeast, and the Sierra de Xichú to the northeast.

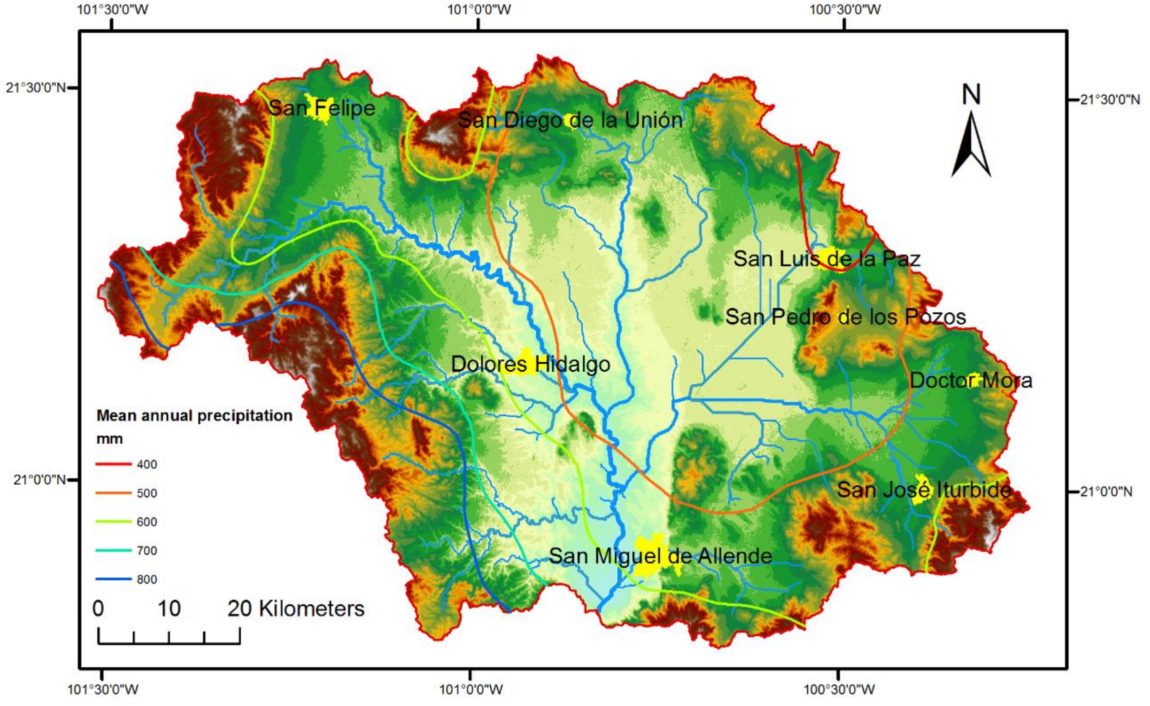

Fig. 1-3 Location of the Independence Basin

1.3.1 Geology

This study area is an intermountain sedimentary basin with complex geology (Aranda-Gómez et al., 2003), filled by Quaternary to Tertiary sediments and covered by phaeozems and vertisols, while the mountain areas are composed of Tertiary felsic volcanic rocks or Cretaceous and Jurassic rocks. Three geological provinces intersect at the Independence Basin: the Sierra Madre Occidental (SMOc); Sierra Madre Oriental (SMOr); and the Transmexican Volcanic Belt (TMVB) (Ferrari et al., 2000; Aranda-Gómez et al., 2003). The oldest rocks in the area are of volcanic, plutonic and volcano sedimentary origin of late Jurassic and early Cretaceous ages. In late Cretaceous a thick sequence of limestones, sandstones, and marls was deposited (SMOr). The sequences are exposed in the east (Sierra de Mineral de Pozos) and southeast (Sierra de los Cuarzos) of the basin. During late Cretaceous and early Tertiary (middle Miocene), voluminous volcanism of intermediate to silicic composition (SMOc) occurred in the north and west of the Independence Basin (Sierra del Cubo and Sierra de Guanajuato).

At least six separate eruptions of rhyolitic ash occurred during the Late Miocene and Pliocene (5–3 Ma) with important volume of andesitic, rhyolitic, and basaltic rocks (TMVB) while the San Miguel Allende basin was subsiding (Adams et al., 2006). During the late Miocene to Pliocene slab breakoff, hot asthenosphere rose through a break in a subducting slab of oceanic lithosphere. Parents of the medium-K series (adakitic magmas) formed as hot rising mantle caused the edge of the torn plate to melt while High-K parental magmas were formed by decompression melting as asthenospheric mantle rose through the gap in the slab. Detailed geologic surveys and different microscopic and analytical techniques were conducted near the San Miguel de Allende region and results showed that erionite-K occurred as a diagenetic product in altered Oligocene–Miocene rhyolitic tuffs, which was formed in the lower part of an open catchment with bicarbonate-rich (T >

30 °C, pH > 8.00) groundwater discharge conditions prevailed in the past (Ortega-Guerrero and Carrasco-Núñez, 2014).

The feet of the mountains are characterized by a sequence of breccias and partially consolidated conglomerates, with blocks and gravels in a matrix of medium to coarse sands whereas the plains consist of gravels, sands, silts, clays and volcanic ashes. The thickness varies from a few meters at the foot of the mountains to 100-460 m in the center of the basin. And the details of the evolution of the Basin and geological descriptions are presented by Alanís-Ruiz, (2002).

1.3.2 Meteorology

Overall, the climate of the Independence Basin is semiarid and the rainfall is not evenly distributed over time nor space with 90.00% of the 600.00 mm mean annual precipitation falling between May and October, of which the majority of rainfall is from June to September. Summer time precipitation is largely generated through interactions between the varied topography and atmospheric circulation cells associated with the North American Monsoon: humid air coming from the Pacific Ocean, as well as the irregular passage of tropical cyclone remnants (Douglas et al., 1993). Typically, as shown in Fig. 1-3, three climate regimes predominate in this research area: in the S and SW of the Sierra de Guanajuato prevails a warm climate with high mean annual precipitation of around 800 mm near the mountainous areas; in the Sierra de Guanajuato and Sierra de San José Iturbide a sub-humid condition is observed; and in the lower parts of the north and east of CI the climate is dry. Additionally, the annual mean temperature is 16 ℃ ranging from 9 to 25 ℃. Evaporation maximizes in summer months with daily values ranging from 1.5 mm in the eastern part of Guanajuato state to 2.00 mm in the western part of the state (Sheffield et al., 2010). The actual evapotranspiration was estimated to be about 518.00 mm/y according to the Turc method (Mahlknecht, 2003). Potential evaporation is more than 1,500.00 mm/y (Barrett and Esquivel Longoria, 2013), and was estimated with a mean value of 1,828.00 mm/y (Navarro De León et al., 2005).

Guanajuato state is also situated at the transition zone under the impact of El Niño-Southern Oscillation (ENSO). Studies have shown that the areas around and to the north of Guanajuato experience little complex variability in summertime precipitation with phase of ENSO (Englehart and Douglas, 2002; Magaña et al., 2003; Barrett and Esquivel Longoria, 2013), nor was there a trend in the frequency of heavy precipitation with daily amounts exceeding the long-term 90th percentile threshold (15.00 mm) not changing from 1979-2011 (Barrett and Esquivel Longoria, 2013). However, Guanajuato does experience variability in extreme precipitation events, including both heavy rainfall and draughts, which was connected to not only ENSO (Ropelewski and Halpert, 1986) but also the Atlantic Multidecadal Oscillation (AMO) (Curtis, 2008; Barrett and Esquivel Longoria, 2013). The maximum temperatures have increased from 1979 to 2011 (Barrett and Esquivel Longoria, 2013): frequency of maximum temperatures exceeding the 90th percentile increased to near 30% while those maximum temperatures below the 10th percentile decreased to near 5.00%. Air temperatures and surface temperatures, sharing the similar variability, were found to be with cooler (warmer) than normal temperatures in the same geographic areas during wetter (drier) precipitation phases. During the period from 2000 to 2009, Guanajuato suffered 68 extreme climatic events: 37 climate events associated with precipitation and the other 31 associated with temperature, respectively (Constantino et al., 2011).

1.3.3 Hydrology and hydrogeology

The mountainsides surrounding the Independence Basin serve as the physical boundary of the watershed with clearly differentiated interfluves. The eastern border reflects as the continental divide, separating the runoffs toward the Gulf of Mexico (Panuco River) and into the Pacific Ocean (Lerma and Santiago rivers), respectively. As shown in Fig. 1-3 the stream net is primarily dendritic corresponding to the local topography. The Laja River is the most important stream in the watershed, extending along the entire length of the basin and serving as the main surface drainage of water flows from all directions of the mountainous areas in the basin. Laja River originates in the sierras of Guanajuato and San Felipe, it flows southeast towards the San Miguel de Allende reservoir passing through Dolores Hidalgo as well as San Miguel de Allende. The main stream accounts for 100 km in length while the branches make up of about 80 km. Two important tributaries also originate from the east Guanajuato sierra towards east to the Laja River. The torrential regime lasts from June to October. However, dams were built at the outlets of these two branches with Alvaro Obregón dam for the northern tributary, Arroyo Dolores Hidalgo, and Peñulitas dam for southern one named as “Erre” or “R” river. The materials in the vicinity of Laja River are constituted by granules with small sizes, indicating good permeability of Laja River (CONAGUA, 2015a), which was verified by the field TEM test (Li et al., 2016). Due to the growing overexploitation of regional aquifers within the watershed, the base flow has disappeared since the 1970s according to a research in 1971 (CONAGUA, 2015a).

Ignacio Allende reservoir is situated at the outlet of the basin and collects the runoffs generated in the basin. As drawn in Fig. 1-5 (a), derived from the 191SM file downloaded from the database of (CONAGUA), the water flow of this whole basin peaked in summer seasons with a crest value over 250.00 m^3/s during the period of 1986-1991. The average runoff recorded at the basin outlet is about 258.00 Mm^3/y. Besides, the storage variation of the reservoir data reveals that the total outlet of runoffs from the entire basin decreased sharply from 2008 with a gradual reduction of peak storage while no significant climatic variation was reported during this period.

It is very likely to have increasing discharge of water flows from the river streams into the shallow alluvial aquifer because the good hydraulic connection (Li et al., 2016).

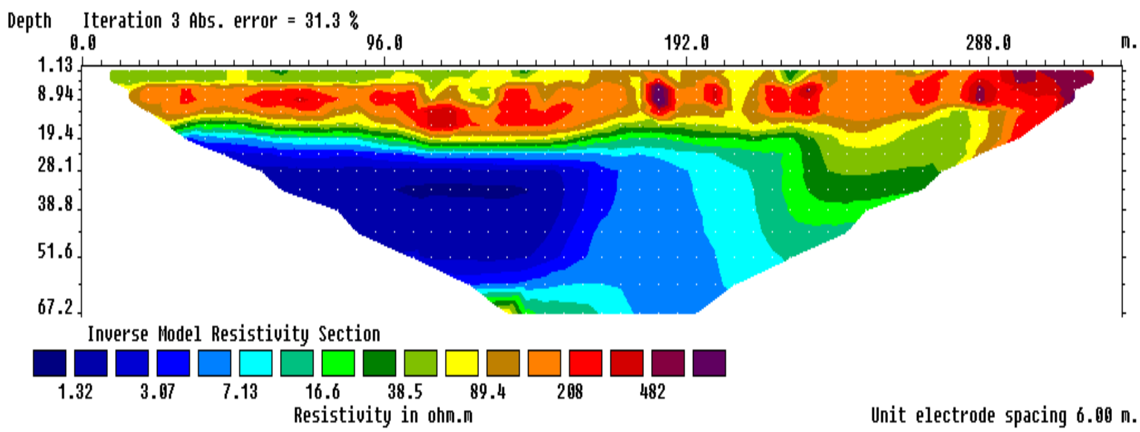

Fig. 1-4 Geophysics properties of Laja River

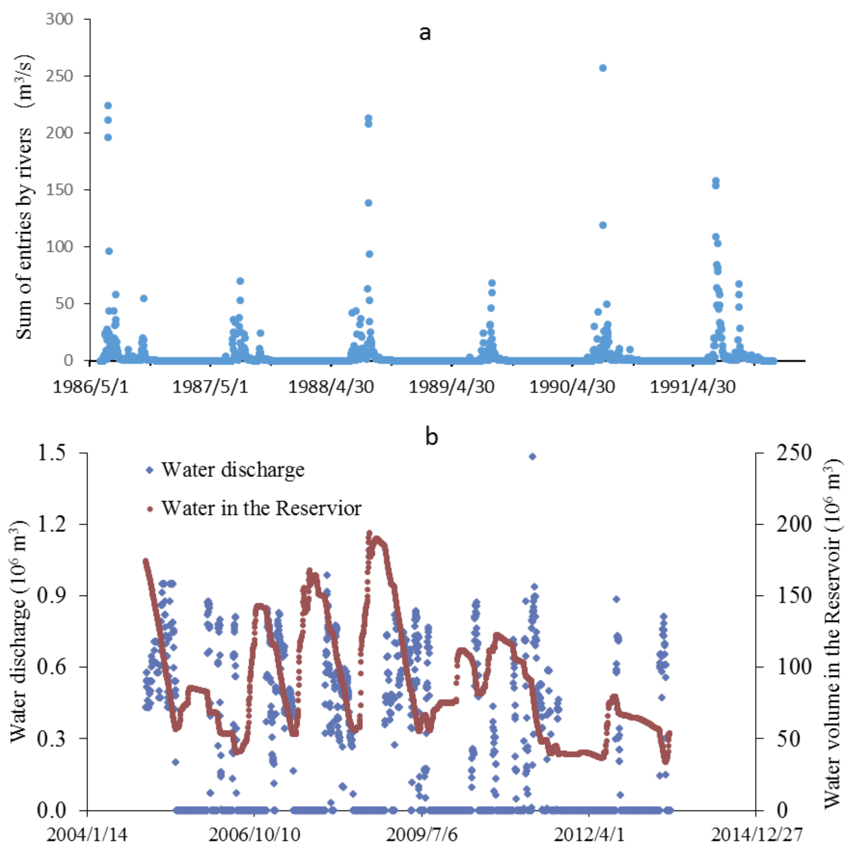

Fig. 1-5 Contribution of river flows (a) and water storage (b) in the Reservoir Ignacio Allende

The aquifer system consists of upper unconsolidated to moderately consolidated basin-fill deposits and lower consolidated, fractured material (Mahlknecht et al., 2006). The basin-fill deposits consist of Pleistocene to Holocene alluvial deposits, and alluvial to lacustrine sandy to silty sediments, interstratified with volcanic conglomerates and tuffs from Pliocene, existing in a thickness of up to 400-500 m. Most of the production wells are drilled in the tuff sequences. The lower fractured aquifer material consists mainly of ignimbrites of rhyolitic origin and plays an important role due to its high fracture density and potential infiltration capacity. Petrographic studies indicate that the siliciclastic aquifer consists mainly of quartz, albite, feldspar, kaolinite, Ca-montmorillonite and hematite (Mahlknecht, 2003). Overall, the hydrogeology of the Independence Basin consists of three hydrostratigraphic units: (a) basal unit of low permeability that performs as an aquiclude made up of sedimentary, volcano sedimentary and plutonic rocks of late Jurassic and early Cretaceous; (b) fractured aquifer composed of marine sedimentary sequences of the late Cretaceous and all the later volcanic emplacements; (c) porous aquifer containing clastic sediments filling the tectonic depressions and forming a vast plain (Navarro De León et al., 2005). A Visual MODFLOW study (Pulido-Madrigal et al., 2012) implemented for a sub-basin located in the northeast (Laguna Seca basin) reveals that the hydraulic conductivity K varies from 0.127 m/d to 2.047 m/d with a medium value of 0.678 m/d. However, the hydraulic conductivity mean values for both aquifers are 2.01 and 4.21 m/d, respectively and the total groundwater recharge calculated in 1991 by water balance approach, is estimated in 170.00 Mm^3/y or 24.90 mm/y (CNA,1992).

The temperatures of groundwater are between 14 °C and 47 °C while the dominant range is from 25 °C to 30 °C (Ortega-Guerrero et al., 2002). These thermal groundwater resources (temperatures above 36 °C) were mostly found in the eastern catchment where the aquifers Laguna

Seca and Dr. Mora - San José Iturbide were located. Additionally, several thermal sites were discovered in the northern part and southern part of the basin, separately.

The hydrogeologic regime in the Independence Basin is a classical gravity-driven flow system with dominance of local, intermediate and regional order, respectively (Navarro De León et al., 2005): (a) area I, located in the mountains and within the plain limits, with cold springs and phreatophytes; (b) area II, located in the central plain, where lagoons, bogs, saline soils and phreatophytes were abundant; and (c) area III, located from the basin center to the basin outlet, in addition to the manifestations previously mentioned, where chalcedony deposits along with thermalism and artesianism phenomena are located. Groundwater recharge comes from rainfall in the mountainous areas near the boundary and discharge in diverse basin regions, depending on the geologic and topographic situation, i.e., the Ground Water Flow Systems (GWFS) convergence coincides with the basin center and continues in the same direction as the surface flow to the basin outlet in the south. The groundwater recharge rate maximizes in the southern highlands over 800 mm/y while minimizes in the plains of the northern part, with 10 mm/y according to the chloride mass balance (CMB) method (Mahlknecht et al., 2004).

Springs, lagoons, wetlands, bogs, saline soils, chalcedony deposits, artesianism, thermalism and phreatophytes are manifestations associated to groundwater discharge in the Independence Basin. The overexploitation of groundwater has caused changes in groundwater flow direction, reduction of the number and discharge of springs and surface waters. The geochemical and isotopic investigation study (Mahlknecht et al., 2006) collected samples from both agricultural and domestic water production wells in this basin, and the ^{3}H, ^{18}O, ^{14}C, ^{13}C were analyzed for the inputs of the geochemical mass-balance code PHREEQC. This study identified the primary recharge areas in this basin based on the environmental isotopes and geochemistry data: mountain-front along the west (Sierra de Guanajuato) and south (Palo Huaerfano and La Joya) and southeast

(Zamorano); and vertical upward flow of the saline water in the northeast (between San Luis de la Paz and San Diego definition la Union). The mountain-front recharge has an age between 2.00-5.00 ka while the recharge water from the Zamorano area is up to 9.00 ka. However, the observed groundwater in the basin center (west from Dolores Hidalgo) is around 11.00 ka. Currently, the heavy groundwater exploitation for irrigation in the Dolores region has provoked the groundwater discharge toward the basin center and consequently flow inversion in the southern part near the Allende dam, where the groundwater was thought to be the same with the surface drainage pattern (Mahlknecht et al., 2004; Mahlknecht et al., 2006).

According to the (IPCC, 2007) report, there is a risk of significant species extinctions in most of central and northern Mexico with replacement of semiarid by arid vegetation under future climate change due to the increases in temperature and associated decreases in soil water, decreasing runoff (by 10.00 to 30.00%). The average surface temperature and precipitation are predicted by increasing of 3-4 ℃ and decreasing about 10 mm during the future period of 2081-2100, respectively (IPCC, 2014). A climate change study implemented in the neighboring state Queretaro predicts that increments in mean annual temperature ranging from 0.8 ℃ to 4.8 ℃ and decrements in mean annual precipitation ranging from 17% to 22%. Which could result in a decline of up to 9.16% in the available water for groundwater recharge and runoff by the end of the 21st century (Herrera-Pantoja and Hiscock, 2015). Though a hydrological study with SWAT model has been implemented in this research area with good simulation of the annual runoffs (Torres-Benites et al., 2005), a systematic hydrological approach to evaluation of groundwater recharge remains to be done.

Chapter 2 Application of SWAT model in the Independence Basin I: Calibration and sensitivity analysis

Water resources management and planning around the world have become a challenging task due to climate change uncertainties in addition to a global concern on its effects in regions suffering from water scarcity (Aeschbach-Hertig and Gleeson, 2012; Molina-Navarro et al., 2016). In arid and semiarid zones that face high inter-annual rainfall variability and scarcity of fresh water, which are commonly associated to extreme events such as floods and droughts, the sustainable use of this resource becomes a priority.

The Independence Basin is situated north of the Guanajuato State with an area of around 7,000.00 km^2 and an elevation range from 1,850.00 to 2,850.00 m, suffering the groundwater scarcity from the over extraction to meet the increasing demands from agricultural irrigation (CEAG, 2014). Evidence of groundwater declining has been recorded by the installed transducers with an annual reduction rate between 1.00 - 3.00 m. Successful catchment management is needed to achieve compromises between conflicting water demands and the sustainable water utilization and social development.

The Soil and Water Assessment Tool (SWAT) model is the most widely used semi-distributed hydrological model, which has been successfully applied to simulate seasonal water and pollutant exports from watersheds in mountainous, plain, and coastal areas of the United States (USA) and other countries around the world, across a range of spatial scales (Nie et al., 2012; Heo et al., 2015; Maier and Dietrich, 2016; Marek et al., 2016). Studies of some sub-basins within Mexico’s territory have been reported , such as the upper San Pedro watershed (Nie et al., 2012), Guadalupe River basin (Molina-Navarro et al., 2016), lake Chapala (Bautista-Avalos et al., 2014), Southwestern Mexico City (Jujnovsky et al., 2012), and also the Independence Basin (Torres-Benites et al., 2005). However, this latter study presented an annual simulation with SWAT for the whole basin without taking into account information about distribution of groundwater recharge. Hence, more work is in demand for evaluation of the streamflow and the groundwater recharge with a shorter time step, and for the assessment of effects induced by potential climate change.

2.1 Description of SWAT model

The SWAT model is a continuous, long-term, physically based semi-distributed model developed to assess impacts of climate and land management on hydrological processes, sediment loading, and pollution transport in watersheds (Arnold et al., 1998). In the SWAT model, a watershed is divided into sub-basins, which are further partitioned into a series of hydrological response units (HRUs). HRUs are uniform units that share unique combinations of soil and land use. Hydrological components, sediment yield, and nutrient cycles are simulated for each HRU and then aggregated for the sub-basins. The hydrological cycle simulated in SWAT is based on the water balance equation:

$$SW_t = SW_0 + \sum_{i=1}^{t} \left(R_{day} - Q_{surf} - E_a - w_{seep} - Q_{gw}\right) \qquad \text{Eq. 2-1}$$

where, SW_t and SW_0 are the final and initial soil water content on day i (mm H_2O), t the time steps on day i, R_{day} the rainfall that reaches the soil surface on day i (mm), Q_{surf} the surface runoff on day i (mm), E_a the evapotranspiration on day i (mm), w_{seep} the interflow on day i (mm), and Q_{gw} is the baseflow on day i (mm) (Neitsch et al., 2011). Schematic structure of water budget is listed in Fig. 2-1 (Neitsch et al., 2011). SWAT simulates hydrological components such as evapotranspiration, canopy storage, mass transport, management practice from input weather data including precipitation, temperatures, solar radiation, wind speed etc. It uses the Soil Conservation

Service curve number (SCS-CN) and the Hargreaves method to estimate runoff and evapotranspiration respectively. For routing the flow, the variable storage routing method was applied.

The Hargreaves method was originally derived from eight years of cool season Alta fescue grass lysimeter data from Davis, California and the form used in SWAT was published in 1985 (Hargreaves and Samani, 1985):

$$\lambda E_0 = 0.0023 \cdot H_0 \cdot (T_{mx} - T_{mn})^{0.5} \cdot (\overline{T_{av}} + 17.8) \qquad \text{Eq. 2-2}$$

where λ is the latent heat of vaporization (MJ/kg), E_0 is the potential evapotranspiraton (mm/d), H_0 is the extraterrestrial radiation (MJ/(m^{2}d)), T_{mx} is the maxim air temperature for a given day (°C), T_{mn} is the minimum air temperature for a given day (°C), and T_{av} is the mean air temperature for a given day (°C).

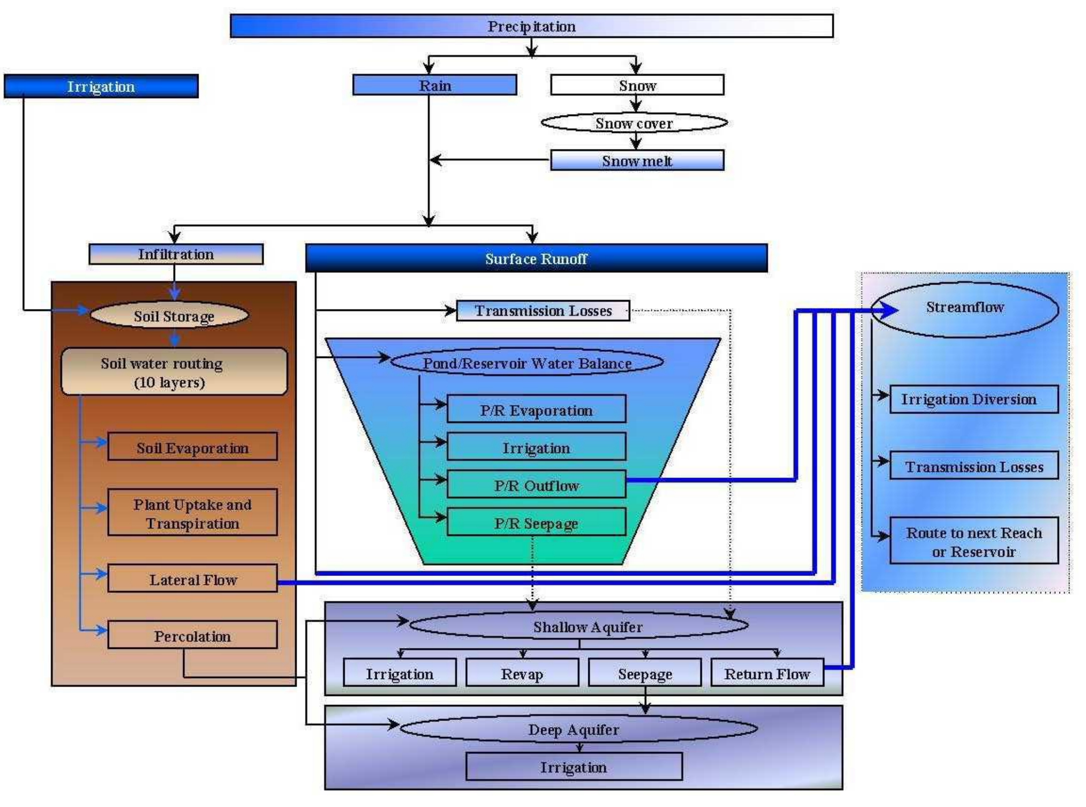

Fig. 2-1 Schematic of pathways available for water movement in SWAT

2.2 Input data for SWAT

In this study, the ArcGIS interface for SWAT, ArcSWAT, version 2012, was used for catchment modeling. Projected coordinate system WGS_1984_UTM_Zone_14N was adopted to ensure the unified coordinate system required by SWAT model. The digital elevation model (DEM) data were obtained from Instituto Nacional de Estadística y Geografía (INEGI), with a resolution of 15×15 m, shown in Fig. 2-2. Soil map was downloaded from Harmonized World Soil Database v 1.2 (Fischer et al., 2008) with resolution of 1 km (Fig. 2-3). Three *soils* were found in this study area, Haplic Phaeozems (PHh), Petric Calcisols (CLp), Haplic Calcisols (CLh), respectively, where PHh and CLp dominate in this area. Soil parameters were transformed from the FAO-90 into USDA standards, whereas soil properties required by SWAT model were calculated using the software SPAW (Soil-Plant-Air-Water Field & Pond Hydrology, version 6.02.75, USDA) with Soil equations defined by (Saxton and Rawls, 2006). A land use coverage map was provided by Instituto de Ecología del Estado, Guanajuato, version 2014 (Fig. 2-4). All the defined land use types were converted into SWAT LUCCs by means of a reference look-up table, as listed in Table 2-1. Temporary/rain-fed agriculture, pasture and irrigated agriculture are three major land coverage types in this area, occupying 26.15%, 25.70% and 17.17%, respectively. Slope was divided into 2 classes, 0-20% and >20%. Soil layer numbers were set to 1 where slopes were greater than 20%. The subdivision into hydrological response units (HRUs, unique computational units of land coverage and soil types with homogeneous hydrologic response) was performed with the aid of land use, soil and slope maps.

Daily meteorological data were obtained from Servicio Meteorológico Nacional (SMN), (Mexican Meteorological Service), extracted into series by Excel automatically. Among the stations available in the selected study sub-basins, those with a coinciding time series long enough to show climate variability and in a period with availability of streamflow data were selected. These weather stations were: San Felipe (SMN), Cienega de Negros, La Quemada, El Carbon, Cañada de Gonzalez, Peñuelitas, Cinco Señores etc. as shown in Fig. 2-2, which ensured a good geographical coverage of the study area. Precipitation, maximum and minimum temperatures were collected, and the missing values were replaced by the default value -99.00 for ArcSWAT model, which will automatically fill missing data with the simulated values during the model running. The reference stations for the weather generator of the model was built with historical statistic data from SMN, Mexico, as well as the aid of SWAT Precipitation Input Preprocessors (pcpSTAT, available from http://swat.tamu.edu/software/links/) recommended by the developers. External reference stations employed in this research area were available from the Climate Forecast System Reanalysis (CFSR) program completed by the National Centers for Environmental Prediction (NCEP), US (http://globalweather.tamu.edu/), with a period over 36 years.

Hydrological gauging data are necessary for model calibration and validation. Available hydrological data from CONAGUA, of 2 stream gauging stations - Puente Dolores and Cinco Señores, and 2 reservoir storage - Peñuelitas and Ignacio Allende, were extracted with VBA codes from CONAGUA's data files. Datasets were prepared in monthly series for different periods. Hence, the whole Independence Basin was calibrated on sub-basin scale at the controlling outlets of Puente Dolores, Peñuelitas and Cinco Señores individually and the rest area, mainly the eastern part of the whole basin, was calibrated by the controlling outlet at Ignacio Allende dam. These 4 gauging stations are shown in Fig. 2-2. In the mountainous areas and the northern part of Independence Basin, reservoirs were set up to delineate the relative sub-basins, and information about these reservoirs were obtained from Seguí (2003), CONAGUA as well as from the Internet. Missing values were calculated from the reference reservoir data. For lacking data of reservoir operations, the outflow was set up with average annual release rates calculated by the SWAT model automatically.

Dominant crops in this area are corn, wheat, beans and alfalfa, which consumed around 90% of extracted annual volume of 412.00 Mm^3 groundwater in the 1970s according to a SARH report (CONAGUA, 2015a). In the study, to simulate the annual groundwater extraction for irrigation, the irrigated crop in SWAT model was replaced by alfalfa. Auto fertilization and auto irrigation were applied to these crops. Irrigation water resources were pumped from the reservoir nearby or directly from deep aquifer within its sub-basin. In the mountainous sub-basins, precipitation lapse rate was set to be 300.00 mm H_2O/km for the selected sub-basins in the west part, while it was 150.00 mm H_2O/km in the east base on the statistical reality that the precipitation decreases from the west towards the east.

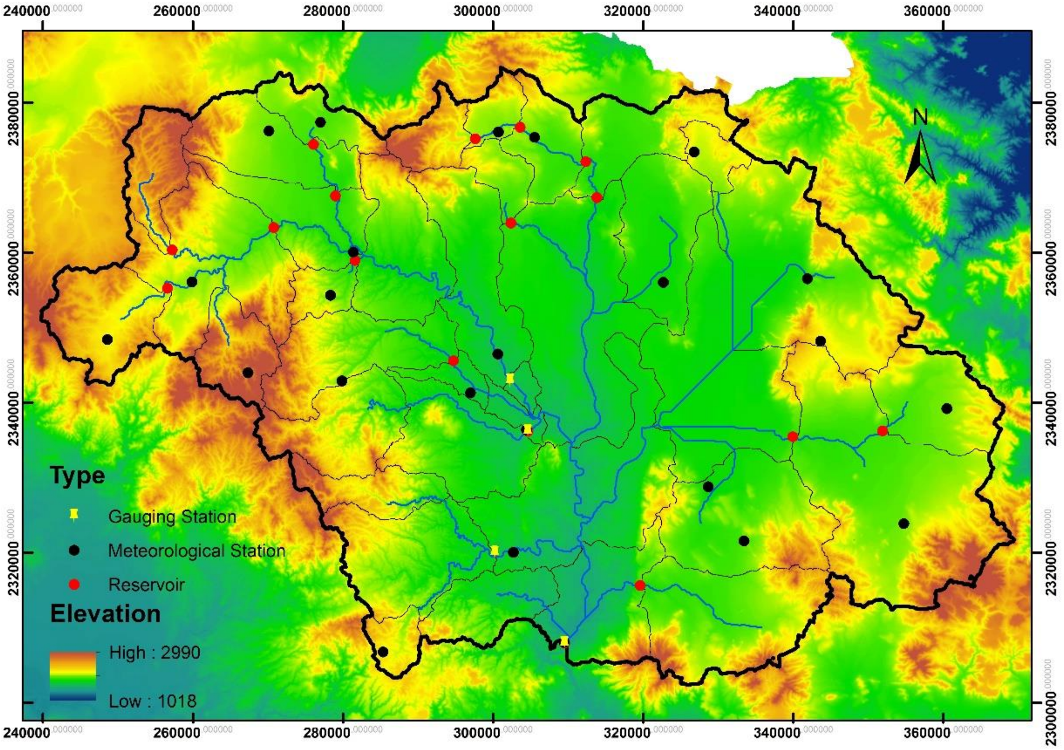

Fig. 2-2 The DEM of the Independence Basin

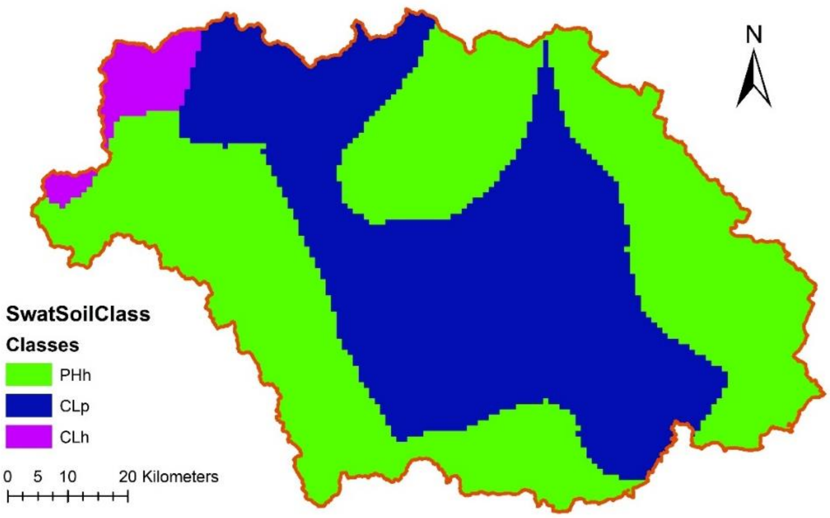

Fig. 2-3 Soil map from HWSD dataset, FAO

Table 2-1 Conversion of land use types into SWAT reference code

Land use type	SWAT reference code	Percentage (%)
Agricultura de riego	AGRC	17.17
Agricultura de temporal	AGRR	26.15
Asentamiento humano	URBN	3.71
Bosque de coníferas	FRSE	1.96
Bosque de coníferas con vegetación secundaria		
Bosque de coníferas y quercus	FRST	2.35
Bosque de coníferas y quercus con vegetación secundaria		
Bosque de quercus	FRSD	9.30
Bosque de quercus con vegetación secundaria		
Cuerpo de agua	WATR	0.97
Matorral xerófilo	RNGB	12.28
Matorral xerófilo con vegetación secundaria		
Pastizal inducido	PAST	25.70
Pastizal natural		
Área sin vegetación aparente	BARR	0.41

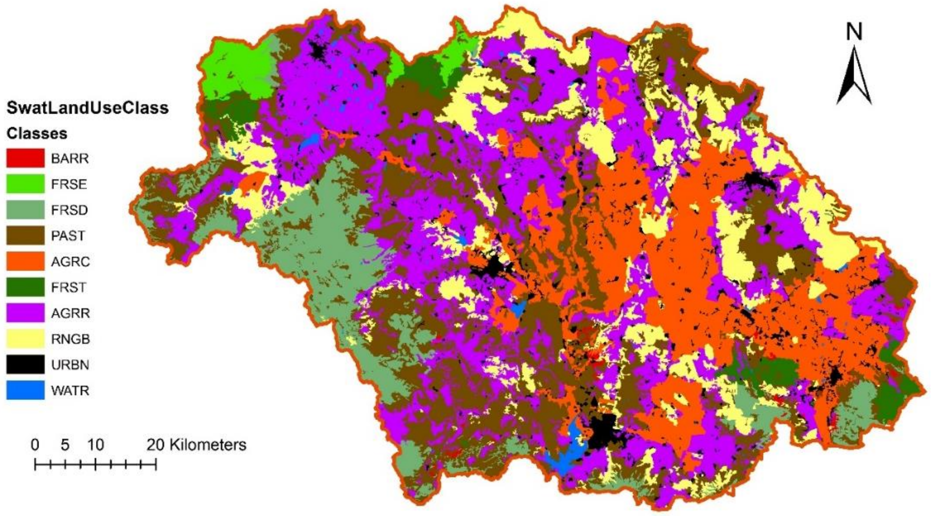

Fig. 2-4 Reclassified land use from Instituto de Ecología del Estado, Guanajuato

2.3 Set-up of the ArcSWAT model

With all the data ready, SWAT model was built within the interface of ArcMap 10.1 as follows:

1) Automatic Watershed Delineation with the DEM data and the favorable gauging sites, and calculation of parameters;

2) HRU definition after the inputs of land use coverage, soil map and slope definition;

3) Weather database construction and weather data input selection, then writing of all the input data into the model database file;

4) Adjustment of parameters for model simulation following recommendations from user's manual and expert consultation;

5) Determination of modeling period, time-step, method and options for output;

6) Simulation and reading the outputs.

In this study, the Independence Basin was delineated into 36 sub-basins and 671 HRUs based on the datasets of gauging stations, reservoirs, land use and slope. As a result, 21 meteorological stations were read by SWAT model for hydrological modeling.

2.4 Model calibration, validation and sensitivity analysis

Parameters of SWAT models are varied at different spatial levels: HRUs, sub-basins and basin. Since sub-catchments may have different basin characteristics, assigning the same basin parameter values to the whole catchment may limit the calibration process. In order to allow each sub-catchment to have its specific basin parameter values and to avoid the limitation of calibration process, sub-basins were calibrated individually. Model calibration and uncertainty analysis for both approaches were carried out by SWAT - CUP: SWAT Calibration and Uncertainty Programs (Eawag, version 5.1.6, 2015), with the Sequential Uncertainty Fitting (SUFI-2) module, which uses a global search procedure through Latin Hypercube sampling. The procedure estimated optimum parameter ranges and carried out global sensitivity analysis for simulating the outputs for consecutive iterations. SUFI2 varies the model parameters with a pre-determined range until the model output best matches observed data and it needs lower amount of model runs to achieve a satisfactory solution compared to other uncertainty analysis techniques, which makes it an attractive method; the alternative of direct measurements of model parameters describing physical systems is often time consuming, expensive and potentially error-ridden (Ficklin et al., 2013). Besides, SUFI2 method was able to provide more reasonable and balanced predictive results than the other two methods (GLUE and ParaSol) assembled in the SWAT-CUP module (Wu and Chen, 2015).

Model performance can also be evaluated by different statistical criteria to compare the simulated data with the measured ones. The coefficient of determination (R^2) and Nash-Sutcliffe Efficiency (*NSE*) objective functions are the two most commonly reported approaches in the current literature. R^2 indicates strength of linear relationship between the observed and simulated values. It ranges from 0 to 1 with 1 indicating the perfect model. *NSE* is a normalized statistic that determines the relative magnitude of the residual variance ("noise") compared to the measured data variance ("information") (Nash and Sutcliffe, 1970). *NSE* indicates how well the plot of observed versus simulated data fits the 1:1 line. It ranges between -∞ and 1, with *NSE* = 1 being the optimal value. The model performance was considered satisfactory when R^2 and *NSE* were greater than 0.50 for flow (Moriasi et al., 2007). PBIAS, underestimating the average tendency of the calibrated data to be larger or smaller than the observed ones, is used as an indicator for model performance (Gupta et al., 1999). The optimum value is zero for an exact model prediction, and so, low absolute values indicate better simulations. At monthly time step, a PBIAS less than 25% for stream flow after calibration is considered satisfactory (Moriasi et al., 2007). General information about assessment criteria is listed in Table 2-2 (Moriasi et al., 2007; Rocha et al., 2015).

The coefficient of determination (R^2) and Nash-Sutcliffe Efficiency (*NSE*) objective functions were used for evaluating the model performances as follows:

$$R^2 = \frac{\left[\sum_i \left(Q_{m,i} - \bar{Q}_m\right)\left(Q_{s,i} - \bar{Q}_s\right)\right]^2}{\sum_i \left(Q_{m,i} - \bar{Q}_m\right)^2 \sum_i \left(Q_{s,i} - \bar{Q}_s\right)^2} \qquad \text{Eq. 2-3}$$

where Q is a variable (e.g., discharge), and m and s stand for measured and simulated, respectively, i is the i^{th} measured or simulated data, and the bar stands for average. If there is more than one variable, then the objective function is defined as:

$$\mathrm{g} = \sum_j w_j R_j^2 \qquad \text{Eq. 2-4}$$

where w_j is the weight of j^{th} variable.

$$NSE = 1 - \frac{\sum_i (Q_m - Q_s)_i^2}{\sum_i (Q_{m,i} - \bar{Q}_m)^2} \quad \text{Eq. 2-5}$$

where Q is a variable (e.g., discharge), and m and s stand for measured and simulated, respectively, and the bar stands for average. If there is more than one variable, then the objective function is defined as:

$$g = \sum_i w_j NS_j \quad \text{Eq. 2-6}$$

where w_j is the weight of j^{th} variable.

$$\text{PBIAS} = \frac{\sum_{i=1}^{n} (O_i - C_i) * 100}{\sum_{i=1}^{n} O_i} \quad \text{Eq. 2-7}$$

where O refers to the observed data while C represents the calibrated values.

Table 2-2 General performance ratings for statistical methods

Performance rating	NSE	PBIAS %	R^2
Very good	>0.75	< ±10	>0.75
Good	0.65 ~ 0.75	±10 ~ ±15	0.65 ~ 0.75
Satisfactory	0.50 ~ 0.65	±15 ~ ±25	0.50 ~ 0.65
Unsatisfactory	≤ 0.50	≥ ±25	≤ 0.50

The sensitivity analysis for the 15 hydrological parameters listed in Table 2-4, was done for the study period (1963-2011), in accordance with the whole calibration period for 1,000 simulations using the global sensitivity analysis by SWAT-CUP. Parameter sensitivities are determined by calculating the following multiple regression system, which regresses the Latin hypercube generated parameters against the objective function values:

$$g = \alpha + \sum_{i=1}^{m} \beta_i b_i \quad \text{Eq. 2-8}$$

A t-test is then used to identify the relative significance of each parameter b_i. The sensitivities given above are estimates of the average changes in the objective function resulting from changes of one individual parameter, while all other parameters are not changed. This gives relative sensitivities based on linear approximations and, hence, only provides partial information about the sensitivity of the objective function to model parameters. The p-value for each term tests the null hypothesis that the coefficient is equal to zero (no effect). A low p-value (<0.05) indicates to reject the null hypothesis. Conversely, a larger p-value suggests that changes in the predictor are not associated with changes in the response, so that parameter is not very sensitive. A p-value of < 0.05 is the generally accepted point at which to reject the null hypothesis (i.e., the coefficient of that parameter is different from 0). In this analysis, the larger, in absolute value, the value of t-stat, and the smaller the p-value, the more sensitive the parameter.

2.5 Results and discussions

A warm-up period of 2 years for the model was executed prior simulation. During model calibration, hydrological parameters were varied within their recommended ranges to match the simulated streamflow with the observed one. The optimum parameter values are listed in Table 2-4. The comparison between simulated and observed monthly streamflow in different periods of calibration and validation for these 4 gauging stations are shown in Fig. 2-5, and the statistical results are listed in Table 2-3. Generally, a good match can be seen between the simulated and observed values by the reference criteria listed previously in Table 2-2.

For the northern part of the Independence Basin, the performance evaluation of the SWAT model for monthly time steps is considered to have a good level. The monthly NSE, R^2 and PBIAS at the outlet of Puente Dolores were respectively, 0.69, 0.72 and -7.80% for the calibration period; while the values were 0.65, 0.66 and -18.6% for NSE, R^2 and PBIAS, respectively, for the validation period. Within this catchment, the water body contributes to about 1.40% of the area with several reservoirs, as well as plenty of ponds which exceeds the maximum area allowed in SWAT model. Additionally, the Jesús María reservoir was constructed in 1991 with total volume

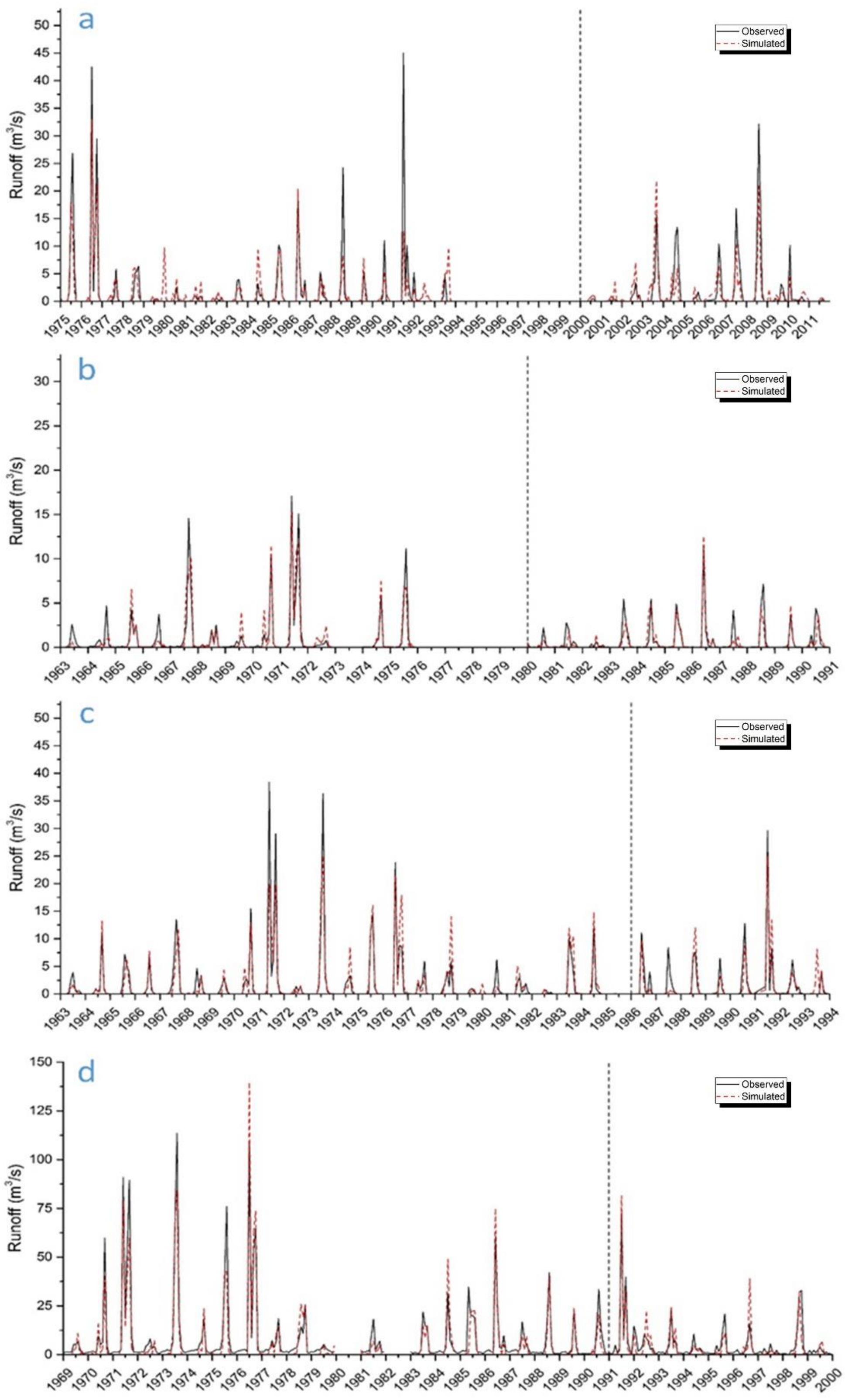

Fig. 2-5 Comparison of observed and simulated monthly runoff at the outlets of a) Puente Dolores, b) Peñuelitas, c) Cinco Señores and d) Ignacio Allende

of 24.00 Mm^3, aimed to irrigate the 2,100.00 hectares of croplands (GTO, 2012). Very good results are obtained in the sub-catchment Cinco Señores, where the *NSE* values are greater than 0.75 for the calibration period as well as the validation period. And its PBIAS values also have a very good level. In its neighbor sub-catchment, Peñuelitas, the performance of the model has a very good-level for NSE, R^2 and PBIAS for the calibration period, while the performance degrades in the validation period, especially for the assessment criteria PBIAS. After the calibration of the western and northern parts of the Independence Basin, the rest was calibrated as a whole by the controlling outlet at Ignacio Allende. Very good results of NSE and R^2 were obtained for calibration and validation periods, but PBIAS criteria was calculated to be acceptable at a level around -20.00%.

Table 2-3 Calibration and validation statistics at the outputs of Independence Basin

Outlet	Simulation Period	NSE	R2	PBIAS%
Puente Dolores	Calibration for 1975-1993	0.69	0.72	-7.80
	Validation for 2000-2011	0.65	0.66	-18.60
Peñuelitas	Calibration for 1963-1975	0.84	0.84	-3.80
	Validation for 1980-1990	0.73	0.74	-16.20
Cinco Señores	Calibration for 1963-1985	0.8	0.81	-2.50
	Validation for 1986-1993	0.78	0.78	-9.10
Ignacio Allende	Calibration for 1969-1990	0.88	0.89	-19.40
	Validation for 1991-1999	0.78	0.82	-20.90

Overall, the SWAT model performs better in the calibration period than that in the validation period as observed in these 4 outlets. As seen from the outlets at Cinco Señores and Ignacio Allende, better performance of SWAT model was obtained in the southern part of the Independence Basin where topographic difference is more mild. Besides, the discrete blanks in precipitation series could lead to the inaccurate estimation of runoff by SWAT. Method is needed to fill the blanks with correlation with reference from the neighbor weather stations and the annual statistics. Precipitation in rainy seasons tends to be in the form of thunderstorms in the afternoon, which makes the SWAT model unable to consider the effects of duration and intensity of precipitation in the areal extension of summer thunderstorms; nevertheless, successful application of SWAT model in runoff estimation has been achieved for the Independence Basin.

A total of 15 parameters, as listed in Table 2-4, were selected for optimization based on literature review on potential sensitive parameters of the SWAT model and the model documentation, which are mostly related to surface runoff and baseflow (Arnold et al., 2000; Arnold et al., 2012). As documented in numerous studies using Soil Conservation Service curve number (CN2) for surface runoff estimation, CN2 is extremely sensitive, and it was in this study too. Other parameters showing high sensitivity were saturated hydraulic conductivity for soil layers (SOL_K), soil available water capacity (SOL_AWC), the threshold water depth in the shallow aquifer for return flow (GWQMN) and the depth from soil surface to bottom of layer (SOL_Z), which were followed by the groundwater 'revap' coefficient (GW_REVAP). The SOL_K, despite being a soil parameter, has a connection with groundwater since it is an indicator for water moving through the soil layers, which will eventually reach in the shallow aquifer below.

The high sensitivity of SOL_K and GWQMN reveals that the groundwater system plays a vital role in the hydrology of the Independence Basin with seasonal climate and Quaternary aquifers. The p-value of SOL_AWC, SOL_Z and the soil evaporation compensation factor (ESCO), which goes along with the importance of evaporation, indicates that evapotranspiration plays an important role in this semi-arid area as well. The similar sensitivity analysis of results have been found in other semi-arid catchments (Mosbahi et al., 2015; Solaymani and Gosain, 2015; Molina-Navarro et al., 2016).

Table 2-4 List of parameters used for model calibration and sensitivity analysis by SUFI2 in SWAT-CUP

No.	Parameter	Min_value	Max_value	Fitted value	t-stat	p-value	Ranking
1	Curve number for moisture condition α, R__CN2.mgt	-0.5	0	-0.43 ~ -0.03	5.25	0.00	1
2	Soil available water capacity, R__SOL_AWC(..).sol	-0.5	0.5	-0.05 ~ 0.46	3.17	0.00	3
3	Saturated hydraulic conductivity for soil layers, R__SOL_K(..).sol	-0.5	0.5	-0.31 ~ 0.40	3.57	0.00	2
4	Depth from soil surface to bottom of layer, R__SOL_Z(..).sol	-0.5	0.5	-0.46 ~ 0.15	2.34	0.02	5
5	Manning's n value for the main channel, R__CH_N2.rte	-0.2	1	-0.16 ~ 0.97	-0.12	0.91	14
6	Effective hydraulic conductivity in main channel, V__CH_K2.rte	0	30	6.23 ~ 15.71	-1.45	0.15	7
7	Baseflow alpha factor, V__ALPHA_BF.gw	0.2	0.95	0.2 ~ 0.79	-0.06	0.95	15
8	Ground water delay time, V__GW_DELAY.gw	2	60	4 ~ 27	0.14	0.89	13
9	Threshold water depth in the shallow aquifer for return flow, V__GWQMN.gw	200	2000	360 ~ 802	2.62	0.01	4
10	Groundwater 'revap' coefficient, V__GW_REVAP.gw	0.02	0.2	0.02 ~ 0.18	-1.67	0.10	6
11	Deep aquifer percolation coefficient, R__RCHRG_DP.gw	-0.5	0.5	-0.44 ~ 0.05	-0.14	0.89	12
12	Threshold depth of Water in the shallow aquifer for 'revap' or percolation to the deep aquifer to occur, V__REVAPMN.gw	100	2000	243 ~ 1629	-0.36	0.72	11
13	Soil evaporation compensation factor, R__ESCO.hru	-0.5	0.5	-0.49 ~ 0.26	-1.00	0.32	8
14	Plant uptake compensation factor, R__EPCO.hru	-0.3	0	-0.26 ~ -0.17	-0.54	0.59	10
15	Precipitation lapse rate, R__PLAPS.sub	-0.5	0.5	-0.12 ~ 0.15	-0.56	0.58	9

*: R_ represents the existing parameter value is multiplied by (1 + *a* given value) while V_ means the parameter is replaced by a given value.

The initial and calibrated values of the adjusted parameters are given in Table 2-4. The baseflow alpha factor (ALPHA_BF) varies from 0.20 to 0.79 in the Independence Basin, indicating that the response to recharge is spatially uneven. According to the theoretical documentation of SWAT (Neitsch et al., 2011), ALPHA_BF values vary from 0.10 to 0.30 for land with slow response to recharge, up to 0.90 -1.00 for lands with a rapid response. Briefly, the ALPHA_BF has an intermediate value in the northern part of the basin, and a low value in the catchment of Peñuelitas, while in the south and east parts of the Independence Basin it has higher values, which correspond to the alluvial aquifers in this area. CH_K2 is set with the default value of 0 in the model, which is recommended to be increased in the semi-arid area in Mexico for water lose from stream bed (Nie et al., 2012; Molina-Navarro et al., 2016). The calibrated CH_K2 ranges from 6.23 to 15.71 mm/hr, which corresponds to the gravel and sand bedded Laja River with good connection to the alluvial aquifer below (Li et al., 2016). CN2 was reduced in the whole basin, with a reduction of less than 10% percent in the north area and around 43% in the south. The GWQMN decreases from the north to the south, meaning that it is easier for groundwater to flow back to reach the southern zone.

2.6 Historical water budgets with SWAT model

After the calibration, the SWAT model was used to simulate the water pathways in the Independence Basin for a 40-year historical period of 1970 - 2009 with updated parameters. The annual results of water pathways as well as the average temperature have been listed in Table 2-5. And the monthly statistical results of precipitation and temperature have been presented in Fig. 2-6 and Fig. 2-7, respectively. Precipitation is the main water source for the whole area with an average accumulated value of 495.10 mm/y in this semi-arid area, and the automatically extracted groundwater by the SWAT model acts as a supplementary source for water input to satisfy the irrigated commercial crops. Among these amounts of water, about 5.80% will become surface runoff and 6.80% will become recharge into the deep aquifer.

Rainfall events mainly occur in the summer season starting from June to September with accumulated precipitation around/over 80.00 mm per month, then it tends to decrease from October. The dry season lasts till the next April. From April to September, the mean temperature remains above 18 ℃ and it peaks at 21 ℃ in May. The difference of monthly mean temperature is 8 ℃. As shown in Fig. 2-9, PET is consistent with the tendency of temperature, which is defined by the Hargreaves method. The annual PET is estimated to be 1,670.00 mm/y, which is higher than the Blaney-Criddle method (Blaney, 1959) with a value of 1,280.00 mm/y. Due to the water availability, the actual evapotranspiration (ET) exists in the similar tendency but having much lower values. Overall, the ET is higher than the accumulated precipitation, which can be attributed to the groundwater pumping activities for agricultural irrigation; while in the rainy season, the ET is less than the precipitation due to the buffering capacity of available water in the soil system. The actual ET is estimated in 473.10 mm/y, which is higher than the Coutagne method (449.00 mm/y), but lower than the Turc's method (518.00 mm/y) (Mahlknecht et al., 2004).

Surface runoff and aquifer recharge mainly occur in the rainy season as can be seen from Fig. 2-12. Annual surface runoff is about 33.38 mm, which is similar to a previous study by (CEASG, 1999) with the same US SCS runoff curve numbers.

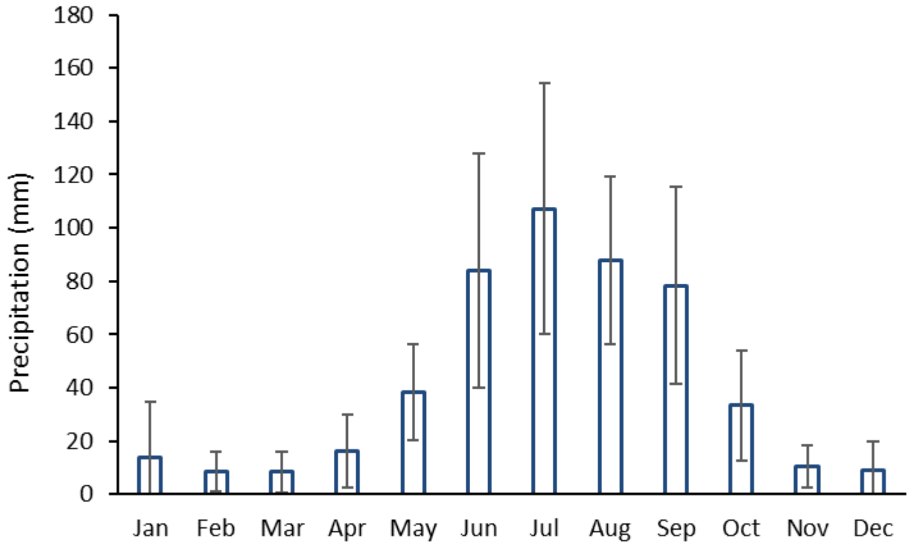

Fig. 2-6 Mean value of monthly precipitation for the past 40 years

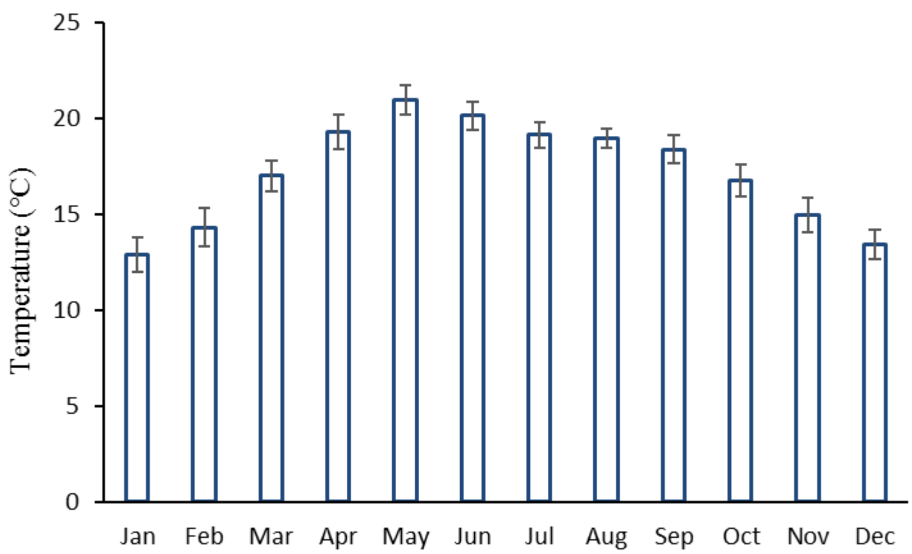

Fig. 2-7 Mean value of monthly temperature for the past 40 years

Table 2-5 Annual statistics of SWAT outputs for the period 1970-2009

Year	Precipitation mm	TMP □	PET mm	ET mm	Runoff mm	Recharge mm	GW Extraction mm
1970	406.5	17.4	1684.6	418.4	35.28	36.21	105.1
1971	651.1	17.0	1630.8	489.6	61.28	87.53	86.80
1972	447.4	17.4	1674.8	476.5	27.56	25.61	90.82
1973	634.7	17.0	1644.6	524.6	56.90	69.64	83.93
1974	385.6	17.0	1677.8	427.9	26.81	17.24	89.13
1975	489.9	16.9	1670.8	472.2	37.27	38.33	90.52
1976	733.1	16.4	1592.5	497.6	67.63	106.8	77.41
1977	470.7	16.8	1651.3	489.6	27.43	31.87	81.55
1978	528.5	16.7	1594.2	473.2	38.86	46.82	81.01
1979	372.7	16.6	1626.4	404.2	18.67	17.94	81.11
1980	465.0	16.9	1623.2	476.8	28.13	29.72	78.89
1981	507.5	16.7	1567.2	511.6	27.74	24.74	71.71
1982	361.4	17.4	1674.5	404.3	18.35	15.54	86.57
1983	439.5	16.9	1636.0	455.0	30.16	27.46	79.77
1984	506.6	16.7	1594.9	463.7	36.49	39.66	77.89
1985	552.6	16.8	1629.6	516.5	39.10	43.38	69.32
1986	565.0	16.9	1613.0	504.5	45.16	42.13	71.55
1987	420.3	16.9	1652.4	430.2	26.91	29.02	77.75
1988	460.7	17.2	1662.1	441.6	32.21	34.10	80.70
1989	434.6	17.2	1682.0	421.1	31.72	33.06	80.25
1990	557.6	17.2	1654.3	533.3	34.98	34.88	75.51
1991	579.4	17.2	1667.3	474.7	46.21	65.32	81.01
1992	609.3	16.7	1614.6	543.3	42.64	51.44	74.44
1993	483.0	17.2	1657.0	460.9	33.42	35.70	79.24
1994	476.8	17.6	1696.3	492.7	25.26	27.85	80.81
1995	473.0	17.8	1690.8	457.7	27.53	35.18	80.30
1996	485.1	17.5	1720.3	449.0	35.25	47.38	86.17
1997	439.3	17.6	1699.4	473.7	20.79	21.77	78.55
1998	485.6	18.0	1759.4	432.2	34.33	51.31	85.93
1999	328.4	17.4	1730.7	384.7	18.55	19.80	90.20
2000	381.1	17.5	1726.4	416.4	19.02	21.21	83.25
2001	426.0	17.7	1719.0	449.4	21.39	26.85	84.65
2002	526.0	17.8	1727.0	503.3	30.48	35.72	80.41
2003	675.4	17.6	1711.2	545.4	53.61	74.79	77.92
2004	587.6	17.7	1725.2	544.1	37.91	42.62	77.88
2005	407.1	17.8	1736.0	444.6	20.34	23.31	86.27
2006	544.9	17.2	1695.9	515.5	36.05	38.07	80.23
2007	550.3	17.5	1716.1	500.8	36.80	47.83	80.71
2008	464.6	17.2	1706.0	453.3	29.34	35.51	85.51
2009	489.4	17.3	1709.8	473.1	28.43	33.02	79.54
Average	495.1	17.2	1670	471.3	33.38	39.08	81.76

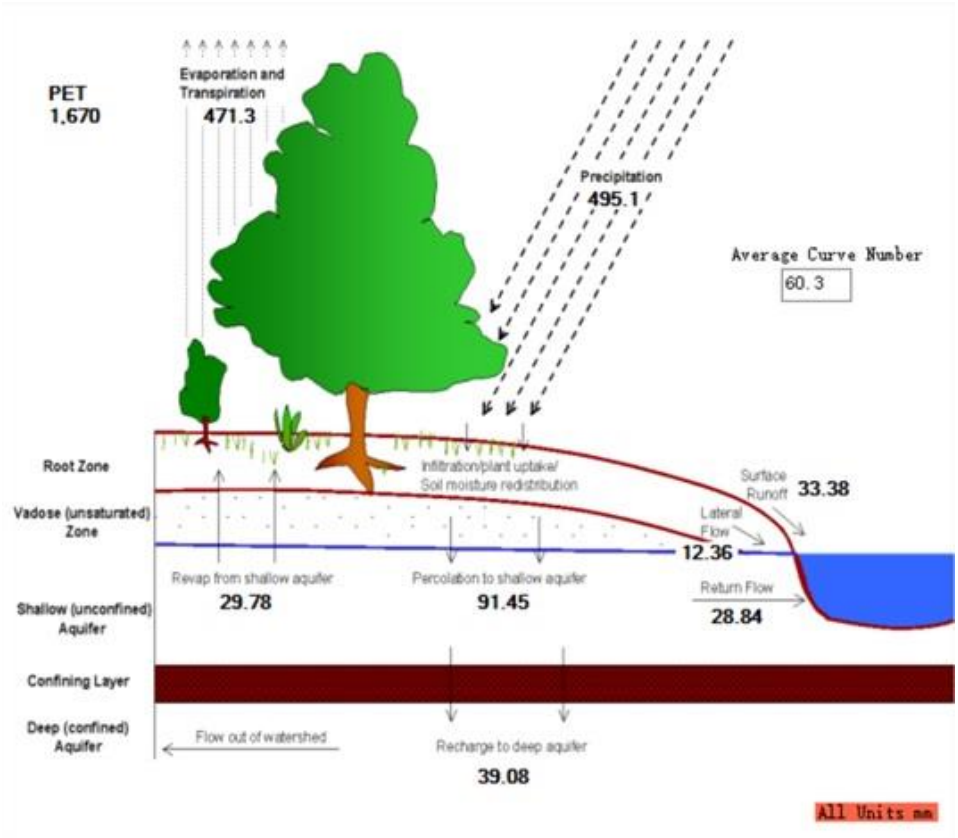

Fig. 2-8 Statistical output by SWAT-Check for the period of 1970-2009

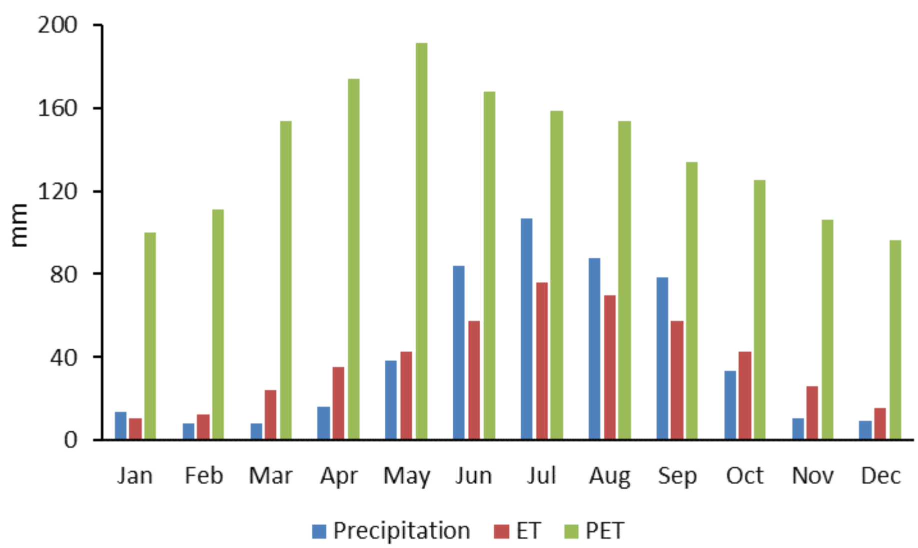

Fig. 2-9 Monthly mean value of precipitation, evapotranspiration and potential evapotranspiration for the period 1970-2009

As documented in Fig. 2-11 and Fig. 2-13, Annual deep aquifer recharge rate fluctuates with the annual precipitation with a mean value of 39.08 mm/y in this study. The reported annual recharge was about 24.90 mm/y by a MODFLOW study in 1992 (Mahlknecht et al., 2004), which is about 40% lower than this study. However, according to the statistical results from CONAGUA Table 2-6, the annual mean recharge is about 296.80 Mm^3/y, i.e. 42.44 mm/y; thus, this study estimates 3.36 mm/y or 7.90% lower than in the CONAGUA's reports. Recharge rate is higher in the western mountainous areas where more rainfall has been received due to the topography (see Fig. 2-10). In the central plain zone and southern-eastern part, the high recharge rate could attribute to the agricultural irrigation activities where are the main irrigating croplands locate. Besides, the high permeability CLp soil would accelerate the water moving towards the alluvial shallow aquifer after rainfall events. As reported in a chloride mass balance (CMB) study by (Mahlknecht et al., 2004), the recharge rate peaks at the western and southern mountainous areas with values over 100.00 mm/y while in the northern part it is less than 50.00 mm/y. In this study, the recharge rate has a similar tendency as the previous study but a higher recharge rate has been found in the central alluvial plain area.

Annual extracted groundwater automatically by SWAT varies from 69.33 mm to 105.12 mm with an average value of 81.46 mm, i.e. 571.72 Mm^3/y. As clearly seen from Fig. 2-11, the recharge rate was equal or similar to groundwater extraction in some years calculated by SWAT model. Though the actual groundwater extraction was lower than 300.00 Mm^3/y in the 1970s, the estimated extracted total volume of groundwater was 520.53 Mm^3 in the year of 1992 when it was assessed to be 487.80 Mm^3 for agricultural irrigation by CONAGUA, (2015b), with an over-estimated portion of 6.70% in this study. Allowed groundwater extraction volume is about 383.40 Mm^3/y but the real case is that extraction is about 832.10

Mm^3/y (see Table 2-6). In consideration of the 90.00% of extracted groundwater consumed by agricultural irrigation, the current study underestimates 23.80% of groundwater extraction in this region in recent years. Then, we could make a conclusion that the deficit of aquifer is worsened in those years with increasing agricultural pumping recently.

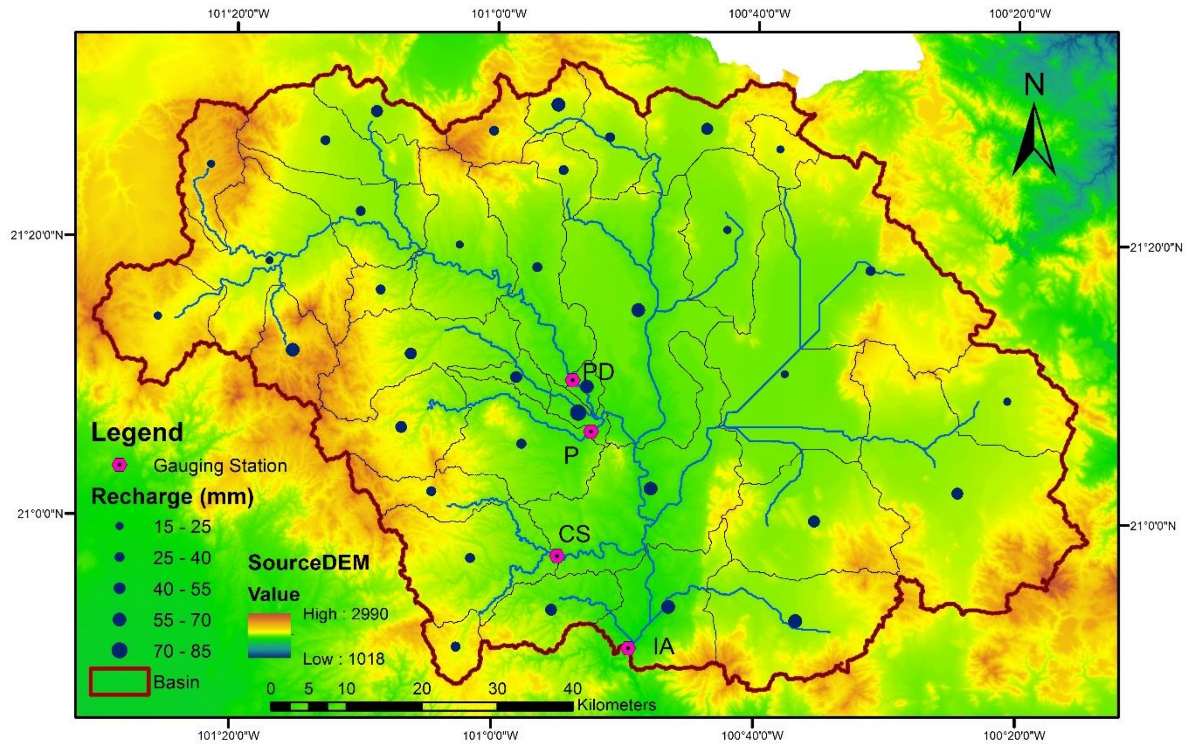

Fig. 2-10 Mean annual recharge into deep aquifer

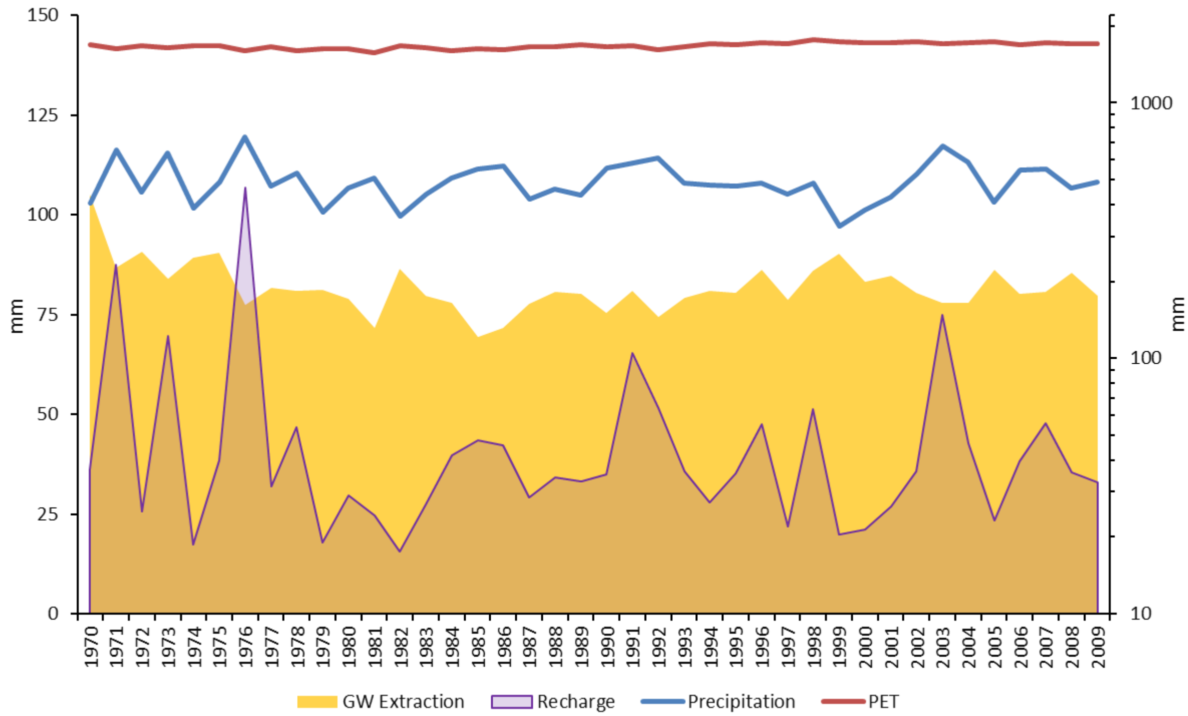

Fig. 2-11 Annual accumulated precipitation, PET, deep aquifer recharge and groundwater extraction, (left vertical axis for recharge and groundwater extraction, and right axis for precipitation and PET)

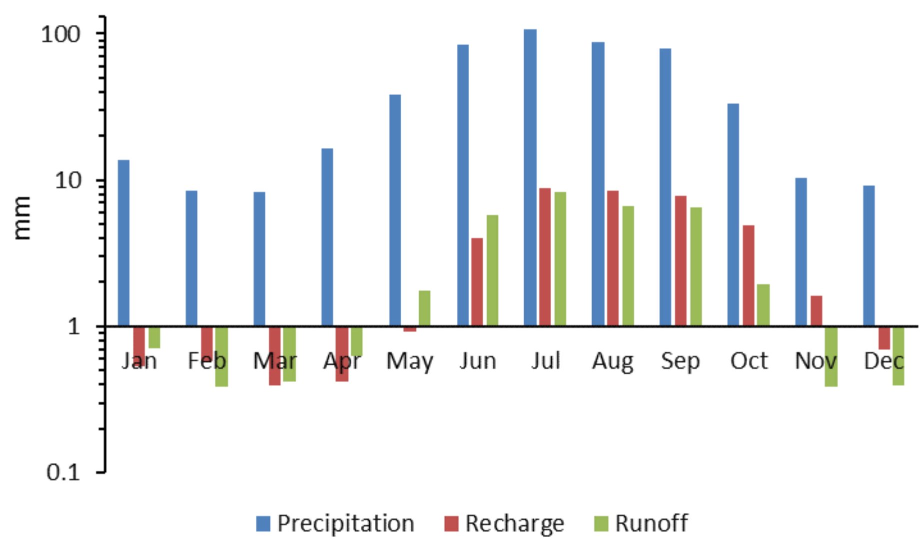

Fig. 2-12 Monthly mean value of precipitation, recharge and surface runoff for the period 1970-2009

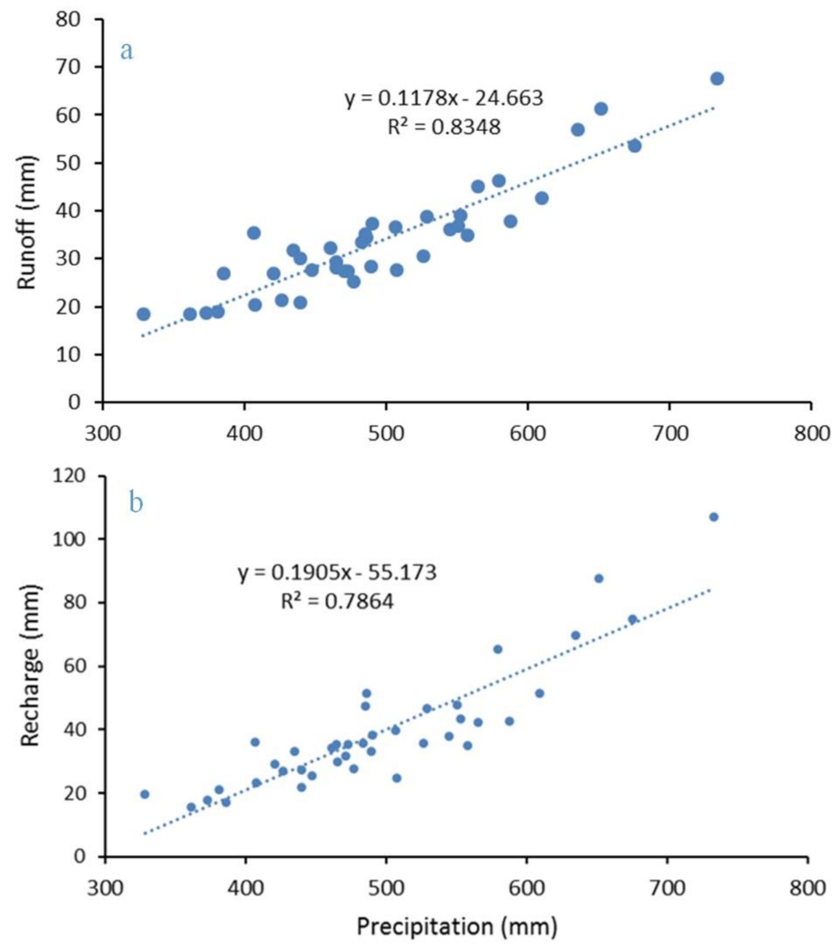

Fig. 2-13 The correlativity between annual a) runoff, b) recharge and precipitation

Table 2-6 Statistical variations of groundwater resources in the Independence Basin (Mm^3/y)

Aquifer	Recharge	Allowed	Extracted	Reference
Alta del Río La Laja	139.7	199.0	412.0	(CONAGUA, 2015a)
Laguna Seca-Dr. Mora	128.5	153.8	398.0	(CONAGUA, 2015b)
San Miguel de Allende	28.6	30.6	22.1	(CONAGUA, 2015c)
Total	296.8	383.4	832.1	

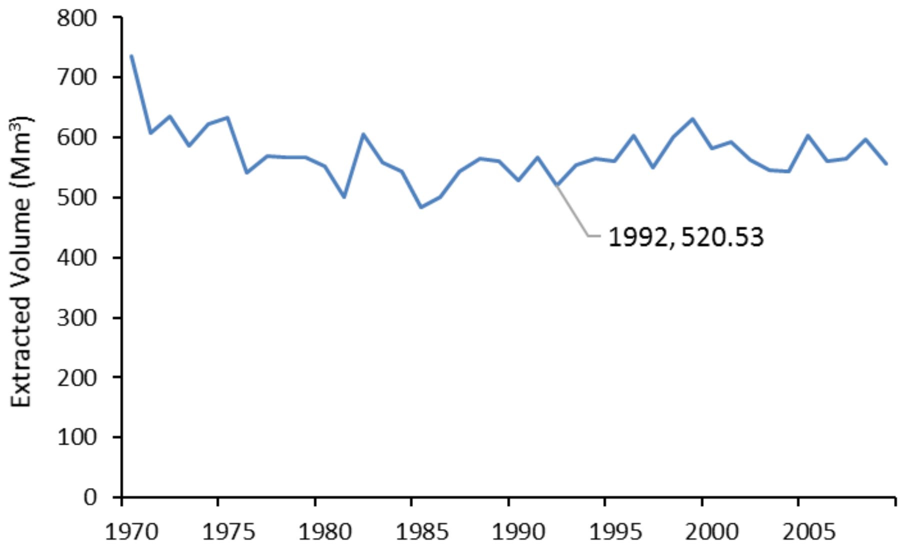

Fig. 2-14 Annual volume of automatically extracted groundwater for agricultural irrigation

2.7 Conclusion

In this chapter, SWAT model is applied to the Independence Basin in the semi-arid area of northern-central of the Mexico Highland, Guanajuato where 36 sub-basins were calibrated with 2 gauging stations and 2 reservoirs records with the aid of SUFI-2 algorithm assembled in SWAT-CUP. In modeling the stream flow, good to very-good results for R^2 (0.66~0.89) and NSE (0.65~0.88) have been obtained during both the calibration and the validation periods, while the PBIAS was not at the level of the former indicators but with satisfactory to very-good results.

As a result of the global sensitivity analysis, CN2, SOL_K, SOL_AWC, GWQMN and SOL_Z were found to be 5 highly sensitive parameters in descending order for the Independence Basin model, indicating that the groundwater system plays an important role in the hydrologic regime. After calibration and sensitivity analysis, a 40-years period of 1970-2009 has been simulated by SWAT with updated parameters. The historical water budget analysis showed the annual precipitation was about 495.10 mm, while PET, ET, deep aquifer recharge and surface runoff were 1,670.00 mm, 471.30 mm, 39.08 mm and 33.38 mm, respectively. The estimated groundwater extraction was lower than the real case, indicating that the drawdown of aquifers has been worsened in recent years.

Chapter 3 Application of SWAT model for the Independence Basin II: Assessing the impacts of future climate change on water resources in the Independence Basin

Climate change is a change in the statistical distribution of weather patterns when that change lasts for an extended period of time (i.e., decades to millions of years) by references to average weather conditions changes, or in the time variation of weather around longer-term average conditions (NRC, 2010). The range of the fluctuations can be regional or global. Climate change is caused by plenty of natural factors such as biotic processes, variations in solar radiation received by Earth, plate tectonics, and volcanic eruptions. Currently, most of the discussions about climate change are related to the environmental policy on the contemporary climate; for that, certain human activities have been identified as significant causes of recent climate change, often referred to as global warming. Since 1950s, many of observed changes are unprecedented over decades to millennia, such as warming atmosphere and ocean, diminishing amounts of snow and ice, the rising sea level. Human influence on the climate system has been proven to be clear for the recent anthropogenic emissions of greenhouse gases (GHG), i.e. carbon dioxide (CO_2), methane (CH_4) and nitrous oxide (N_2O), peaked at the highest level in the last 800,000.00 years (IPCC, 2014). Recent climate changes have had widespread impacts on human and natural systems on all continents and across the oceans.

Anthropogenic GHG emissions are mainly driven by population size, economic activity, lifestyle, energy use, land use patterns, technology and climate policy, upon which the Representative Concentration Pathways (RCPs) describe four different pathways of GHG emissions and atmospheric concentrations, air pollutant emissions and land use for the 21st century. These RCPs consist of a stringent mitigation scenario (RCP 2.6), two intermediate scenarios (RCP 4.5 and RCP 6.0) and one scenario with very high GHG emissions (RCP 8.5). RCP 4.5, developed by the MiniCAM modeling team at the Pacific Northwest National Laboratory's Joint Global Change Research Institute (JGCRI) in the U.S., is a stabilization scenario where total radiative forcing is stabilized at 4.50 W/m^2 (~650.00 ppm CO_2) before 2100 by employment of a range of technologies and strategies for reducing greenhouse gas emissions (Clarke et al., 2007; Wise et al., 2009). The RCP 8.5 is developed by the MESSAGE modeling team and the IIASA Integrated Assessment Framework at the International Institute for Applies Systems Analysis (IIASA), Austria, which is characterized by increasing greenhouse gas emissions over time representative for scenarios in the literature leading to high greenhouse gas concentration levels (Riahi et al., 2007). In the RCP 8.5 emissions scenario the radiative forcing level reaches 8.50 W/m^2, or equal to 1,370.00 ppm CO_2. Relative to the period from 1850 to 1900, global surface temperature change for the end of the 21st century (2081–2100) is projected to likely exceed 1.5°C for RCP 4.5, RCP 6.0 and RCP 8.5 (high confidence). And under the RCP 8.5 scenario, the high latitudes and the equatorial Pacific are likely to experience an increase in annual mean precipitation (IPCC, 2014).

In Mexico's Central Highland, declining rainfall, increasing temperature, decreasing lake levels as well as rising population have been found during the past decades (Orozco-Ramírez and Astier, 2017). Maximum temperature trends have been investigated, resulting in a significant increment in most of ten Mexican watersheds, including Laja and Lerma-Salamanca (Mateos et al., 2016). The daily temperature range exhibits a positive trend (increments), thus implying an increase in temperature extremes. Land-use and land-cover changes could be the main drivers of climate change in the Mexico's Central Highland (Mateos et al., 2016). However, though land use change may influence the hydrological regime in a more identifiable way, in some sub-basins, the future climate change tends to affect the hydrological regimes much more prominently than land use changes (Zhang et al., 2016).

Assessment of the likely impacts of future climate change on water resources is of great importance in order to understand how different sectors could be affected in the Independence Basin by numerous agricultural pumping activities. Furthermore, analyzing the available water resources for the future is fundamental to develop sustainable water management policies and appropriate adaptation strategies that allow for the successful administration of water demand variability.

3.1 Climate change data:

NASA Earth Exchange Global Daily Downscaled Projections (NEX-GDDP) dataset (https://cds.nccs.nasa.gov/nex-gddp/) is comprised of downscaled climate scenarios for the globe that are derived from the GCMs runs conducted under the Coupled Model Intercomparison Project Phase 5 (CMIP5) and across two greenhouse gas emissions scenarios known as Representative Concentration Pathways (RCPs), i.e. RCP 4.5 and RCP 8.5. 7 GCMs, listed in Table 3-1, were selected with downscaled projections for RCP 4.5 and RCP 8.5 from the 21 models and scenarios with high spatial resolution of 25 km. Precipitation, maximum temperature and minimum temperature series in daily intervals have been extracted and processed for 3 30-year periods: 1970-1999, 2030-2059 and 2070-2099, representing the historical baseline scenario, the mid-century and the end of this century, respectively. For the missing precipitation in the period of 2096-2099 for GFDL-CM3 in scenario RCP 4.5, thus the simulation period is shortened to 2070-2095 with 26 years for it.

Table 3-1 CMIP5 model sources

Model	Center	Country
BCC-CSM1.1	Beijing Climate Center	China
CanESM2	Canadian Centre for Climate Modelling and Analysis	Canada
CCSM4	National Center for Atmospheric Research	USA
CNRM-CM5	Centre National de Recherches Météorologiques, Centre Européen de Recherche et de Formation Avancée en Calcul Scientifique	France
CSIRO-MK3.6.0	Commonwealth Scientific and Industrial Research Organization/Queensland Climate Change Centre of Excellence	Australia
GFDL-CM3	Geophysical Fluid Dynamics Laboratory	USA
MRI-CGCM3	Meteorological Research Institute	Japan

3.2 Baseline scenario

The calibrated model was used to simulate the water budget for the baseline condition (1970-1999) with observed data, as shown in Table 3-2, Table 3-3 and Fig. 3-1.. Briefly, annual precipitation, PET, ET, surface runoff, deep aquifer recharge and temperature are 491.70 mm, 1,654.40 mm, 466.90 mm, 34.14 mm, 39.47 mm and 17.1 ℃, respectively. More details can be found in the previous chapter. Monthly precipitation and temperature of 7 GCMs for the baseline have been listed in Table 3-2 and Table 3-3 , while the annual statistics of other parameters are listed in Table 3-4. The mean annual precipitation from the 7 GCMs is 495.80 mm/y, a little bit higher than the observed data. Less precipitation has been generated in the dry season from November to April and more rainfall will be received during the rainy season. All these 7 GCMs are consistent with moderate variations, which can be seen in Fig. 3-2. For the temperature in Fig. 3-3, the difference of annual mean temperature is about 0.3 ℃ between the observed data and modeled ones.

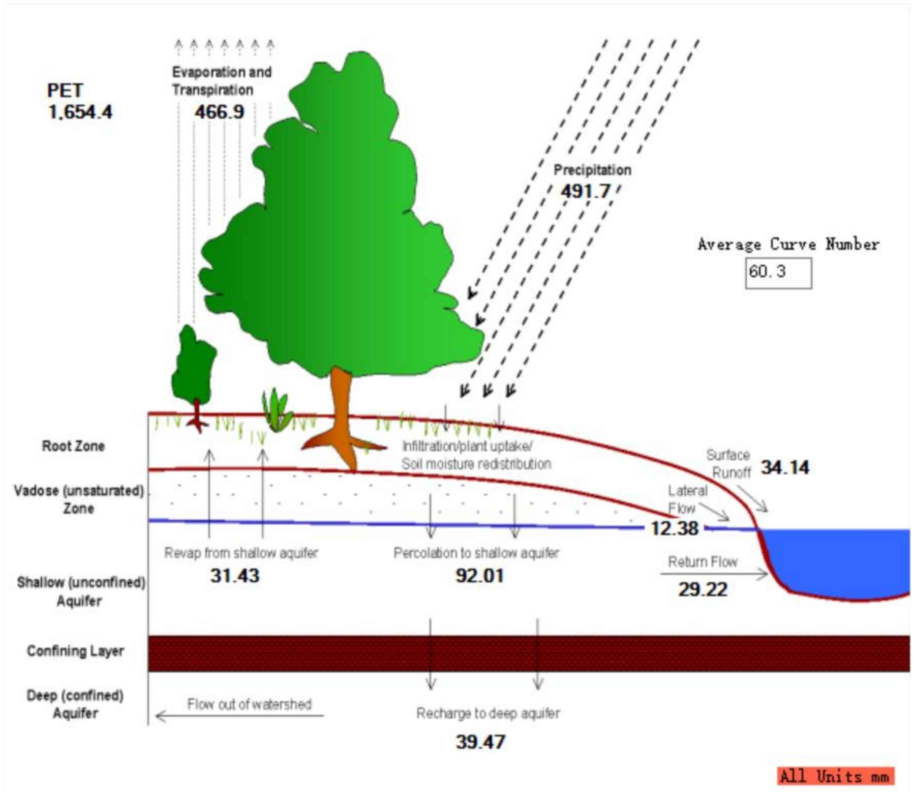

Fig. 3-1 Annual statistical outputs of the reference period 1970-1999 with measured data

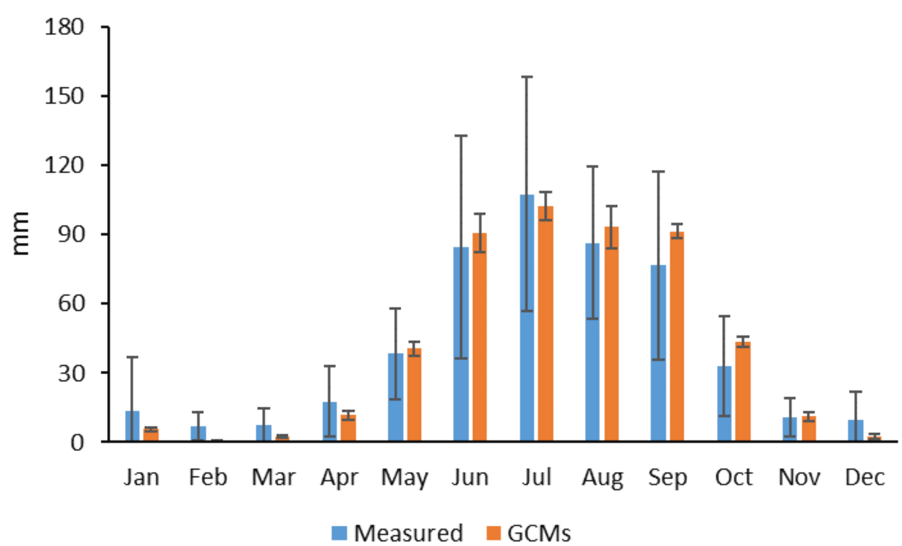

Fig. 3-2 Comparison of monthly precipitation between measured data and models for the period of 1970-1999

Table 3-2 Average accumulated precipitation (mm) for the baseline condition (1970-1999 period)

	Measured	BCC-CSM1.1	CanESM2	CCSM4	CNRM-CM5	CSIRO-MK3.6.0	GFDL-CM3	MRI-CGCM3
Jan	13.54	6.31	5.81	4.71	6.17	5.67	5.2	4.97
Feb	6.99	0.42	0.47	0.47	0.49	0.55	0.56	0.85
Mar	7.52	1.79	1.76	2.41	1.71	3.42	2.77	2.09
Apr	17.65	15.42	11.11	11.23	11.43	13.25	10.61	9.39
May	38.26	44.24	38.33	41.67	43.29	41.61	38.37	36.18
Jun	84.48	89.82	94.49	84.71	93.47	75.76	98.33	99.12
Jul	107.41	91.87	100.58	103.54	110.83	104.66	99.17	107.17
Aug	86.37	91.61	108.81	82.67	89.44	101.76	93.25	85.97
Sep	76.58	84.82	91.15	93.77	91.1	92.86	94.15	91.69
Oct	32.79	40.87	41.8	43.76	45.21	43.24	42.65	46.77
Nov	10.56	10.65	13.03	9.24	8.83	11.46	11.07	13.29
Dec	9.54	2.96	2.06	1.52	1.64	3.75	3.84	1.37
Annual	491.69	480.78	509.4	479.7	503.61	497.99	499.97	498.86

Table 3-3 Average temperature (°C) for the baseline condition (1970-1999 period)

	Measured	BCC-CSM1.1	CanESM2	CCSM4	CNRM-CM5	CSIRO-MK3.6.0	GFDL-CM3	MRI-CGCM3
Jan	12.8	13.6	13.3	13.6	13.5	13.2	13.3	13.2
Feb	14.1	15	15.1	15.1	14.9	15.1	15.3	15.1
Mar	17	17.4	17.5	17.4	17.4	17.3	17	17.5
Apr	19.2	19.5	19.6	19.6	19.5	19.4	19.4	19.7
May	21	20.9	21	21.1	21	20.8	20.9	21
Jun	20.1	20.3	20.4	20.5	20.2	20.4	20.1	20.2
Jul	19	19.5	19.5	19.6	19.4	19.4	19.3	19.5
Aug	18.9	19.6	19.5	19.5	19.6	19.4	19.4	19.4
Sep	18.2	18.5	18.5	18.5	18.5	18.6	18.5	18.5
Oct	16.6	17	17.1	17.3	17.1	16.9	17	17.1
Nov	14.9	15.7	15.5	15.6	15.4	15.5	15.3	15.3
Dec	13.4	13.9	13.9	13.7	13.7	13.7	13.5	13.6
Annual	17.1	17.6	17.6	17.6	17.5	17.5	17.4	17.5

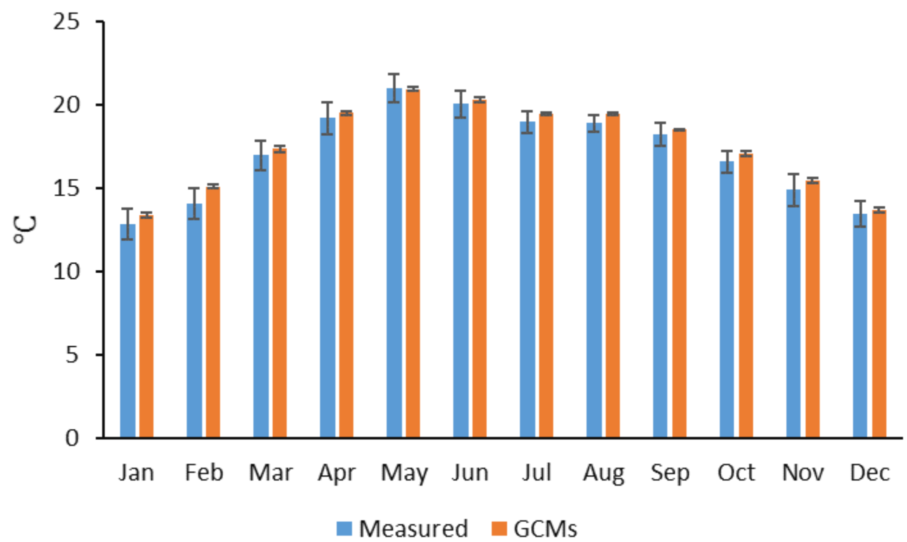

Fig. 3-3 Comparison of monthly temperatures between measured data and models for the period of 1970-1999

Table 3-4 Average outputs for the baseline condition (1970-1999 period) (mm)

Model	PET	ET	Surf Q	Lat Q	Water Yield	Recharge	Extraction	Deficit
Measured	1654.4	466.9	34.14	12.38	115.22	39.47	81.8	42.33
BCC-CSM1.1	1651.2	498.8	21.3	9.7	85.82	32.18	81.43	49.25
CanESM2	1648.8	524	21.84	10.16	88.03	32.5	78.59	46.09
CCSM4	1656	457	31.53	11.06	114.94	42.7	82.16	39.46
CNRM-CM5	1642.9	481	30.76	11.53	115.47	43.35	81.73	38.38
CSIRO-MK3.6.0	1641.2	489.9	26.78	10.87	103.87	38.71	80.11	41.4
GFDL-CM3	1633.3	487.4	28.9	10.71	108.82	40.88	80.71	39.83
MRI-CGCM3	1640.6	466	32.77	11.55	121.69	45.92	80.79	34.87
Average[a]	1644.9	486.3	27.7	10.8	105.52	39.46	80.79	41.33

*[a]: average value for 7 GCMs.

3.3 Future meteorological projections

Variation of GCM projections clearly demonstrated that climate predictions were not uniform in the direction and magnitude of changes for both future study periods (2030-2059 and 2070-2099), as can be seen from Fig. 3-4 and Fig. 3-5. Compared to their own historical scenarios, these GCMs predicted similar precipitation variation tendency in the period of 2030-2059 and that of 2070-2099 under the RCP 4.5 emission scenario. All these models predicted less rainfall would occur by the end of this century when compared with the middle period of this century. In the rainy season, an increasing precipitation would occur in May, June and August to October. In general, the mean annual precipitation will increase by 3.60% and 0.60% for the periods of 2030-3059 and 2070-2099, respectively. Under the RCP 8.5 emission scenario, the monthly variation of precipitation has similar trends to RCP 4.5 emission scenario. Precipitation was projected to increase by 3.80% and 3.40% individually for the periods of 2030-3059 and 2070-2099 when compared to the historical baseline. Comparatively, the neighboring Queretaro River Basin was projected to receive 17.00% - 22.00% less precipitation than the baseline (Herrera-Pantoja and Hiscock, 2015).

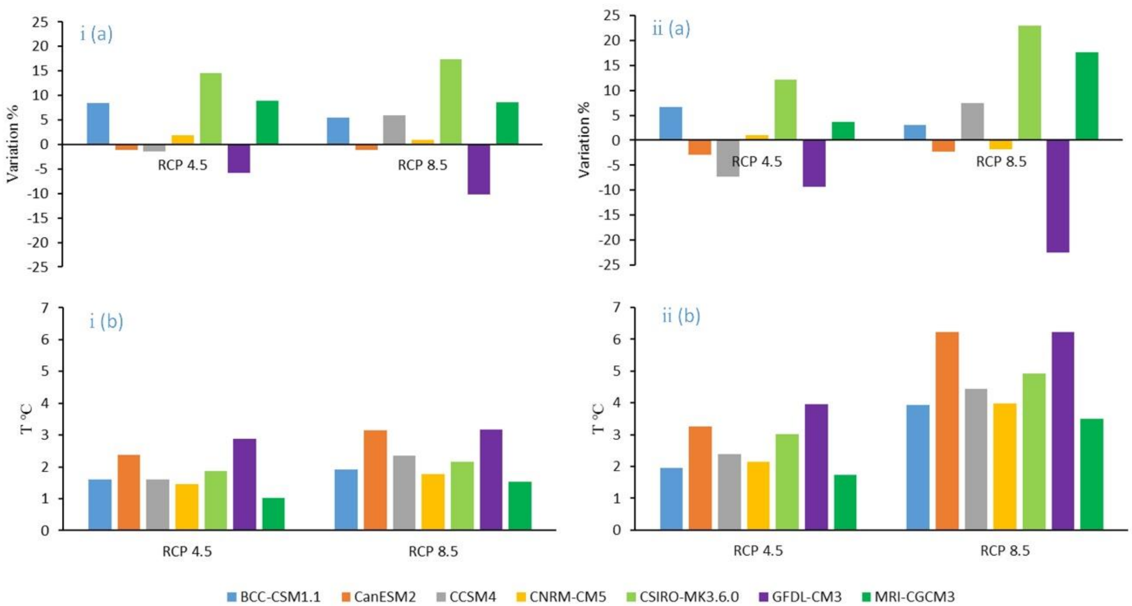

Fig. 3-4 Average annual changes in a) precipitation and b) temperature from baseline for i) (2030-2059) and ii) (2070-2099)

Unlike the fluctuating projection for precipitation, mean temperature was projected to increase in different periods under different emission scenarios by all these 7 GCMs. The mean annual temperature tends to increase by 1.8 ℃ and 2.6 ℃ for the periods of 2030-3059 and 2070-2099 under RCP 4.5 emission scenario, respectively, while by 2.2 ℃ and 4.7 ℃ under RCP 8.5 emission scenario, respectively.

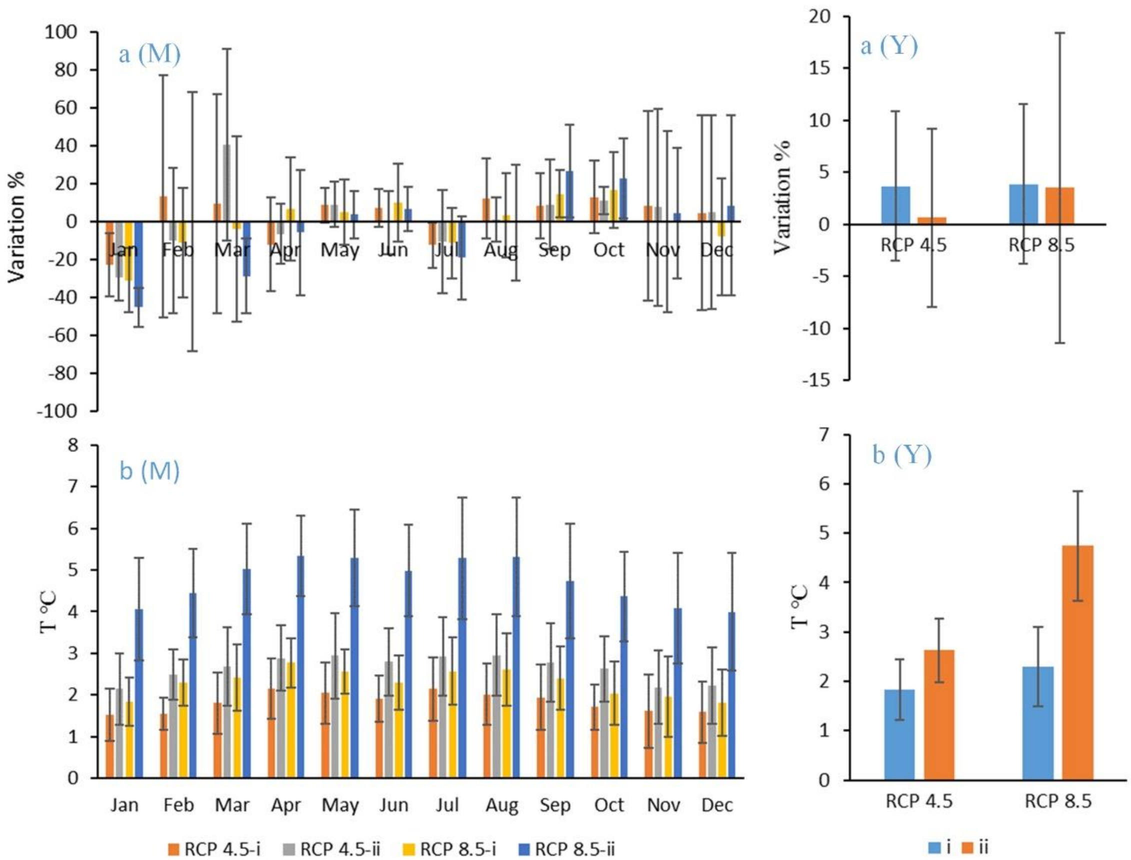

Fig. 3-5 Average monthly (M) and annual (Y) changes of a) precipitation and b) temperature from baseline for i) (2030-2059) and ii) (2070-2099)

3.4 Hydrological response to Climate Change

It is notable that the future projected precipitation varies with different emission scenarios, which is important for the water resources pathways in the Independence Basin. Average monthly PET showed increasing trends for all months under projections of climate change (Fig. 3-6), especially for RCP 8.5 emission scenario when compared to the baseline scenario. It is estimated that annual PET is increasing for all conditions (Fig. 3-7), which can be attributed to the projected increasing temperature as shown previously. On average, annual PET would increase by 6.7% and 9.9% for the periods of 2030-2059 and 2070-2099 under the RCP 4.5 emission scenarios, respectively, while by 8.3% and 17.1%, under the condition of RCP 8.5 emission scenario respectively (Fig. 3-9).

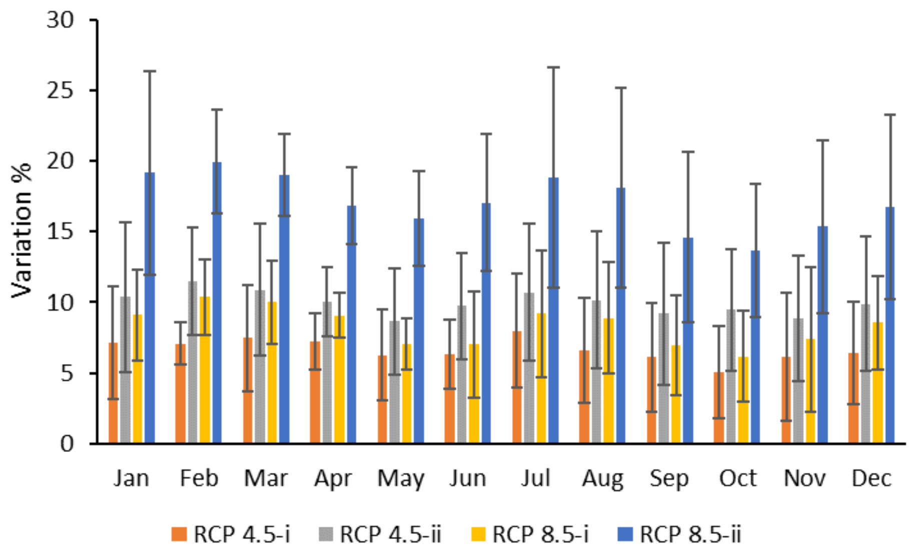

Fig. 3-6 Average monthly changes of PET from baseline for i) (2030-2059) and ii) (2070-2099)

Actual ET is not always increasing as the PET, in some GCMs' projections, it is even estimated to decrease. In the case of BCC-CSM 1.1 model, ET is estimated to be reduced under all conditions. ET tends to stay consistent with the variations of precipitation, which can be seen from the CSIRO-MK 3.6.0 and MRI-CGCM3 predictions. Under the condition of RCP 4.5 emission scenario, ET tends to increase in the period of 2030-2059 and to decrease in the period of 2070-2099 for most models. While under the condition of RCP 8.5 emission scenario, the estimated ET of all the GCMs has a similar tendency in both periods, either to increase or to decline. Besides, the tendency is more noticeable in the period of

2070-2099. Statistically (shown in Fig. 3-9), actual ET tends to increase by 1.6% and 1.3% in the period of 2030-2059 under the emission scenarios of RCP 4.5 and RCP 8.5, respectively. There will be a slightly reduction of ET (-0.4%) in the period of 2070-2099 under RCP 4.5 emission scenario and an increment of 2.1% will occur under the emission scenario of RCP 8.5.

As generated from precipitation, surface runoff has the similar tendency of precipitation events in most GCMs such as BCC-CSM 1.1, CCSM4, CSIRO-MK 3.6.0, GFDL-CM3 and MRI-CGCM 3. Interestingly, the variations of surface runoff are proportionally higher in these models when compared with the corresponding variations of precipitation. In general, surface runoff is estimated to increase 10.5% and 9.2% in the mid-century and at the end of this century under RCP 4.5 emission scenario, respectively. Higher increase of surface runoff is predicted under RCP 8.5 emission scenario with values of 11.8% and 20.2% for those two periods, respectively.

Deep aquifer recharge has similar variations to runoff. As predicted by BCC-CSM 1.1, CSIRO-MK 3.6.0 and MRI-CGCM 3, recharge will increase by 7.3% - 61.5% under conditions of future climate change, while it is simulated with a reduction of 6.3% - 54.5% by CanESM 2 and GFDL-CM3. Averagely (shown in Fig. 3-9), mean annual recharge is simulated to increase by 6.0% and 4.8% in the periods of 2030-2059 and 2070-2099 under RCP 4.5 emission scenario, respectively, while by higher variations of 8.9% and 14.1% respectively in the same periods under RCP 8.5 emission scenario. Significant increasing of groundwater demands for agricultural irrigation are predicted by these GCMs under conditions of future climate change except for the conditions of CSIRO-MK 3.6.0 in the mid-century, which projected 14.5% and 17.3% increments of precipitation under emission scenarios of RCP 4.5 and RCP 8.5, respectively, but just 6% increasing of PET. By the end of this century, there will be sharp growing demands of groundwater extraction, especially under condition of RCP 8.5 emission scenario. Overall, mean annual groundwater extraction, compared with the baseline, has been predicted to increase by 2.3%, 4.3%, 8.4% and 24.2% in the periods of 2030-2059 and 2070-2099 under emission scenarios of RCP 4.5 and RCP 8.5, respectively.

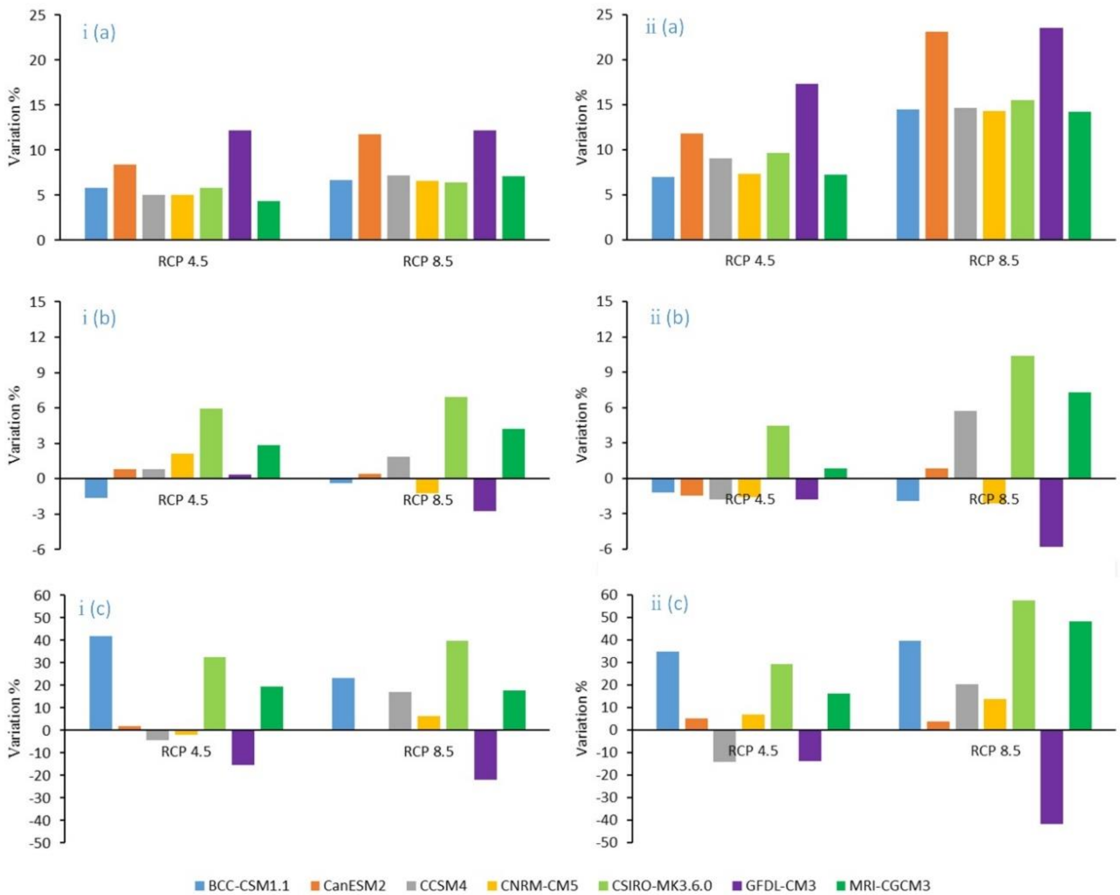

Fig. 3-7 Average annual variations % from baseline in a) PET, b) ET and c) surface runoff for i) (2030-2059) and ii) (2070-2099) in RCP 4.5 and RCP 8.5 climate change scenarios given by 7 GC models.

In this study, aquifer deficit is defined as the gap between groundwater extraction and aquifer recharge (in mm/y). Among predictions of these GCMs, aquifer deficit is likely to rise sharply under simulations CanESM 2 and GFDL-CM 3 when compared to their respective/corresponding baselines, while it will slow down under projections CSIRO-MK

3.6.0 and MRI-CGCM 3. However, there is no chance for the recovering of deep aquifer under the current status of water resources management in the Independence Basin as presented in Fig. 3-8. Statistically (shown in Fig. 3-9), the aquifer deficit rate will remain the same as it currently is in the period of 2030-2059, but it will be augmented in the period of 2070-2099 under both emission scenarios RCP 4.5 and RCP 8.5.

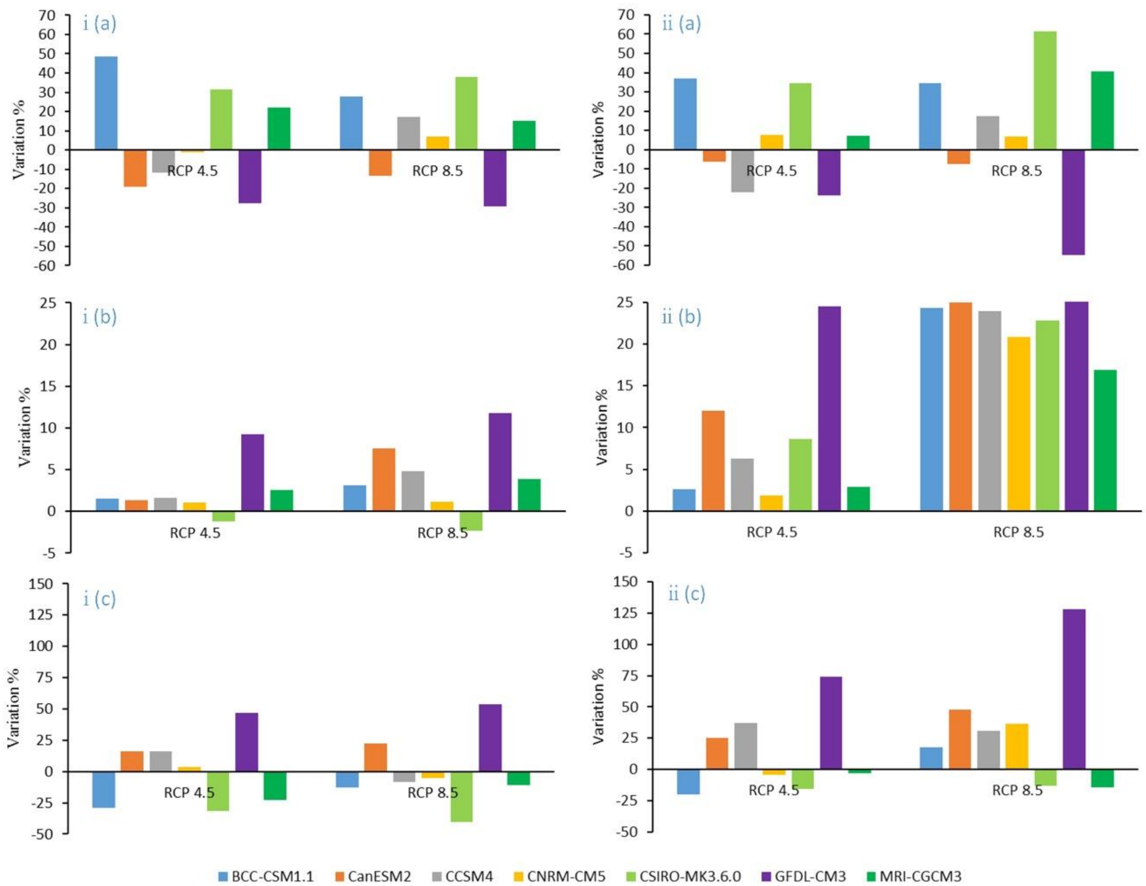

Fig. 3-8 Average annual variations % from baseline in a) recharge, b) groundwater extraction and c) aquifer deficit from baseline for i) (2030-2059) and ii) (2070-2099) in RCP 4.5 and RCP 8.5 climate change scenarios given by 7 GC models.

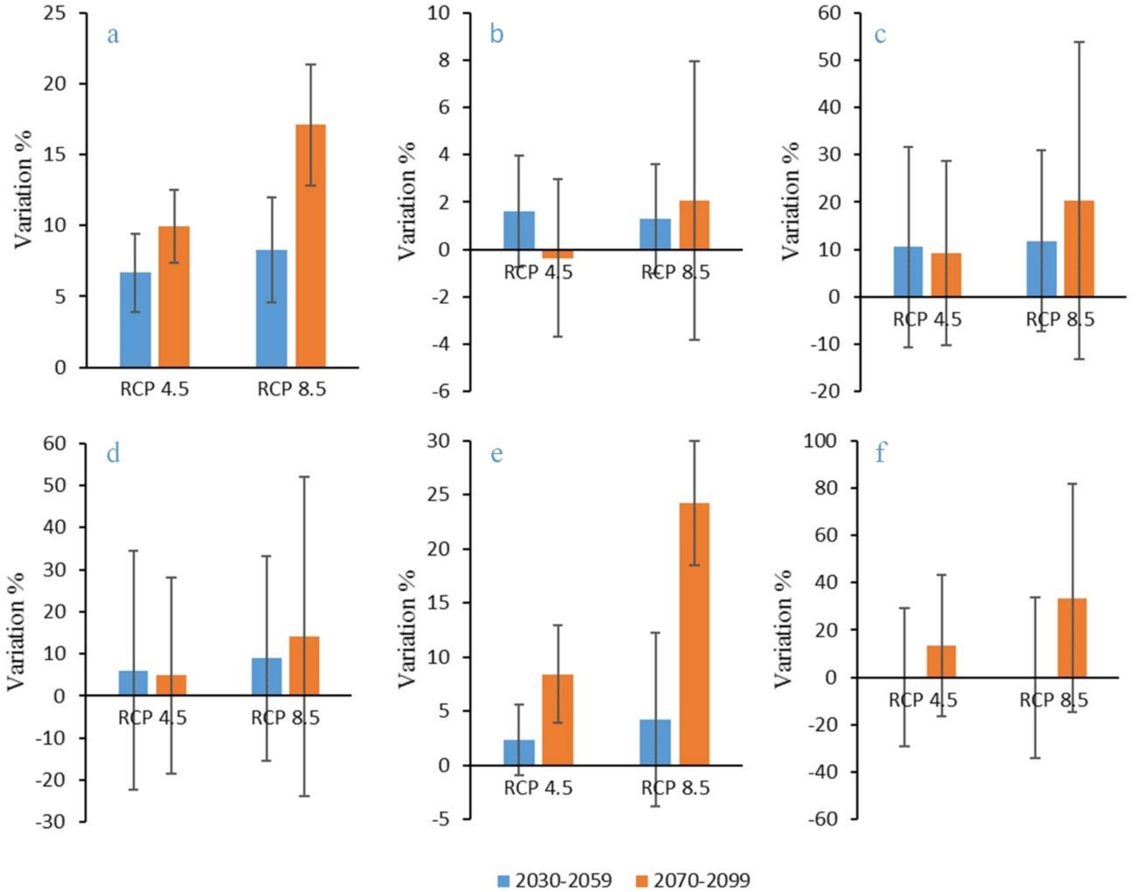

Fig. 3-9 Statistical annual changes in a) PET, b) ET, c) surface runoff, d) recharge, e) groundwater extraction and f) aquifer deficit from baseline for i) (2030-2059) and ii) (2070-2099) for 7 GCMs in different climate change scenarios

3.5 Conclusion

The hydrologic response to climate change was evaluated using SWAT for the semi-arid Independence Basin, Guanajuato, Mexico. Potential climate change conditions were examined under RCP 4.5 and RCP 8.5 emission scenarios for the mid-century (2030-2059) and the end of this century (2070-2099) which were generated by 7 GCMs under CMIP5.

The following conclusions can be drawn from this chapter:

1) According to the projections of 7 GCMs, the Independence Basin may experience higher precipitation and temperature under all emission scenarios for both periods compared to the baseline condition (1970-1999).

2) For future climate change, PET was estimated to increase continuously from 6.7%-8.3% in the period of 2030-2058 to 9.9%-17.1% in the period of 2070-2099, while ET increases at lower rates.

3) Both mean annual surface runoff and deep aquifer recharge was simulated to increase more rapidly under condition of scenario RCP 8.5 than that of RCP 4.5. Under emission scenario of RCP 4.5, the increasing rates of surface recharge and deep aquifer recharge will slow down at the end of this century when compared to the mid-century increasing rates.

4) As induced by the increasing PET, groundwater extraction would increase gradually under current management status. It has been estimated an increasing demand of 8.4% and 24.2% of groundwater exploitation for agricultural irrigation at the end of this century under emission scenarios RCP 4.5 and RCP 8.5, respectively.

5) It has been predicted that no chance of aquifer recovery would happen in the future under the condition of climate change, not even for the most optimistic of the predicted scenarios. As for the drawdown of water table in the Independence Basin, it will remain at the current rate in the mid-century, but it will accelerate at the end of this century.

Chapter 4 Conclusions and recommendations

4.1 Conclusions

In this study, the hydrologic model SWAT was used to evaluate the historical water resources as well as the potential impacts of future climate change on hydrologic regime in the Independence Basin, a semi-arid watershed located at the Central Highland of Mexico. The delineated 36 sub-basins were calibrated with 2 gauging stations and 2 reservoirs datasets with the aid of SUFI-2 algorithm assembled in SWAT-CUP.

Potential climate change conditions were examined under RCP 4.5 and RCP 8.5 emission scenarios for the mid-century (2030-2059) and the end of this century (2070-2099) by 7 GCMs under CMIP5.

The following conclusions can be drawn from this study:

1) In modeling the stream flow, good to very-good results with R^2 (0.66~0.89) and NSE (0.65~0.88) have been obtained during both the calibration period and the validation duration, while the PBIAS was not so good as the former indicators but with satisfactory to very-good results nevertheless.
2) CN2, SOL_K, SOL_AWC, GWQMN and SOL_Z were 5 highly sensitive parameters in descending order in the Independence Basin mathematical model, indicating that the groundwater system plays an important role in the hydrologic regime.
3) The historical water budget analysis of a 40-year period 1970-2009 has been simulated by SWAT with updated parameters, showing that annual precipitation was about 495.1 mm, while PET, ET, deep aquifer recharge and surface runoff were 1670 mm, 471.3 mm, 39.08 mm and 33.38 mm, respectively. The estimated groundwater extraction was lower than the present case, indicating that the drawdown of aquifers has been worsened in recent years.
4) According to the projections of 7 GCMs, the Independence Basin may experience higher

precipitation and temperature under all emission scenarios for both periods, compared to the baseline condition (1970-1999).

5) For future climate change, PET was estimated to increase continuously from 6.7%-8.3% in the period of 2030-2058 to 9.9%-17.1% in the period of 2070-2099, while ET is to increase at lower rates. Both mean annual surface runoff and deep aquifer recharge was simulated to increase more rapidly under condition of scenario RCP 8.5 than that of RCP 4.5. Under emission scenario RCP 4.5, the increasing rates of surface runoff and deep aquifer recharge will slow down at the end of this century when compared to the mid-century rates.

6) As induced by the increasing PET, groundwater extraction would expand gradually under the current management status. It is estimated an increasing demand of 8.4% and 24.2% of groundwater exploitation for agricultural irrigation at the end of this century under emission scenarios RCP 4.5 and RCP 8.5, respectively. It has been predicted that no chance of aquifer recovery would happen in the future under the condition of climate change. As for , the drawdown of water table in the Independence Basin it will remain at the current rate in the mid-century, but it will accelerate at the end of this century.

4.2 Recommendations

Recommendations for possible future studies include:

1) In the current study, the land use was provided by Instituto de Ecología del Estado, Guanajuato with the newest map version to calibrate the SWAT model and to evaluate the impacts of future climate change on hydrology. Nevertheless, all croplands were assumed to cultivate the same crop under the same land use category. Various crop types as well as land use change should be taken into consideration for future model improvement and for assessing the future hydrologic impacts in future studies.

2) Meteorological data, especially precipitation, for model calibration was not sufficient because of missing periods in some meteorological stations. Methods have to be developed to fixing these blanks by interpolation and statistics etc.

3) This study used the SWAT model to evaluate the surface runoff and the groundwater recharge as well. However, the outputs should be further examined by means of groundwater system model simulations or observations. Coupling the SWAT model with MODFLOW is an alternative to improve the SWAT model performance as well as the spatial accuracy of deep aquifer recharge.
4) This study focused mainly on hydrology. Further studies are needed to assess the impacts induced by agricultural management, land use change and climate change on water quality in the Independence Basin, Guanajuato state.

References

Adams Aaron J., Christiansen Eric H., Kowallis Bart J., et al. Contrasting silicic magma series in miocene-pliocene ash deposits in the San Miguel de Allende Graben, Guanajuato, Mexico [J]. The Journal of Geology, 2006, 114(2): 247-266.

Aeschbach-Hertig Werner, Gleeson Tom. Regional strategies for the accelerating global problem of groundwater depletion [J]. Nature Geoscience, 2012, 5: 853-861.

Alanís-Ruiz E. Evolución geológica de la CI y sus alrededores, estado de Guanajuato, México [D]. México, DF: Universidad Nacional Autónoma de México, 2002.

Aranda-Gómez José Jorge, Godchaux Martha M., de Jesús Aguirre-Díaz Gerardo, et al. Three superimposed volcanic arcs in the southern Cordillera-from the Early Cretaceous to the Miocene, Guanajuato, Mexico, 2003 [C].

Arnold J. G., Moriasi D. N., Gassman P. W., et al. SWAT: Model use, calibration, and validation [J]. Transactions of the ASABE, 2012, 55(4): 1491-1508.

Arnold J. G., Muttiah R. S., Srinivasan R., et al. Regional estimation of base flow and groundwater recharge in the Upper Mississippi river basin [J]. Journal of Hydrology, 2000, 227(1-4): 21-40.

Arnold J. G., Srinivasan R., Muttiah R. S., et al. Large area hydrologic modeling and assessment e Part 1: Model development [J].1998.

Barrett B. S., Esquivel Longoria M. I. Variability of precipitation and temperature in Guanajuato, Mexico [J]. Atmósfera, 2013, 26(4): 521-536.

Bautista-Avalos D., Cruz-Cardenas G., Moncayo-Estrada R., et al. Application of the SWAT model to evaluate the diffuse contamination sources at lake Chapala sub-basin, Mexico [J]. REVISTA INTERNACIONAL DE CONTAMINACION AMBIENTAL, 2014, 30(3): 263-274.

Blaney H. F. Monthly Consumptive Use Requirements for Irrigated Crops [J]. Journal of the Irrigation and Drainage Divisio, 1959.

CEAG. http://agua.guanajuato.gob.mx/pdf/agua_subterranea.pdf.

CEAG Comisión Estatal Del Agua. Actualización de modelos de disponibilidad hídrica superficial y subterránea en el Estado de Guanajuato. Guanajuato: 1999.

Clarke Leon, Edmonds James, Jacoby Henry, et al. Scenarios of greenhouse gas emissions and atmospheric concentrations [J]. US Department of Energy Publications, 2007: 6.

CONAGUA Comisión Nacional Del Agua. Banco Nacional de Datos de Aguas Superficiales (BANDAS). http://www.conagua.gob.mx/CONAGUA07/Contenido/Documentos/Portada%20BANDAS.htm.

CONAGUA Comisión Nacional Del Agua. Actualización de la disponibilidad media anual de agua en el acuífero Cuenca Alta del Río La Laja (1108), Estado de Guanajuato. Diario Oficial de la Federación, 2015a.

CONAGUA Comisión Nacional Del Agua. Actualización de la disponibilidad media anual de agua en el acuífero Laguna Seca (1104), Estado de Guanajuato. Diario Oficial de la Federación, 2015b.

CONAGUA Comisión Nacional Del Agua. Actualización de la disponibilidad media anual de agua en el acuífero San Miguel de Allende (1107), Estado de Guanajuato. Diario Oficial de la Federación, 2015c.

Constantino T., Roberto M., Dávila I., et al. Una aproximación a la vulnerabilidad y la resiliencia ante eventos hidrometeorológicos extremos en México [J]. Política y cultura, 2011,(36): 15-44.

Cortés Felipe I. Arreguín, Maravilla Enrique Mejía. Evolution of Water Management in Mexico [J]. International Journal of Water Resources Development, 2011, 27(1): 245-261.

Curtis Scott. The Atlantic multidecadal oscillation and extreme daily precipitation over the US and Mexico during the hurricane season [J]. Climate Dynamics, 2008, 30(4): 343-351.

Döll P., Hoffmann-Dobrev H., Portmann F. T., et al. Impact of water withdrawals from groundwater and surface water on continental water storage variations [J]. Journal of Geodynamics, 2012, 59-60: 143-156.

Douglas Michael W., Maddox Robert A., Howard Kenneth, et al. The mexican monsoon [J]. Journal of Climate, 1993, 6(8): 1665-1677.

Endfield Georgina H., Tejedo Isabel Fernández, O'Hara Sarah L. Conflict and Cooperation: Water, Floods, and Social Response in Colonial Guanajuato, Mexico [J]. Environmental History, 2004, 9(2): 221-247.

Englehart P. J., Douglas A. V. Mexico's summer rainfall patterns: an analysis of regional modes and changes in their teleconnectivity [J]. Atmósfera, 2002, 15(3): 147-164.Ferrari Luca, Conticelli Sandro, Vaggelli Gloria, et al. Late Miocene volcanism and intra-arc tectonics during the early development of the Trans-Mexican Volcanic Belt [J]. Tectonophysics, 2000, 318(1－4): 161-185.

Ficklin Darren L., Luo Yuzhou, Zhang Minghua. Watershed modelling of hydrology and water quality in the Sacramento River watershed, California [J]. Hydrological Processes, 2013, 27(2): 236-250.

Fischer G., Nachtergaele F., Prieler S., et al. Global Agro-ecological Zones Assessment for Agriculture (GAEZ 2008). IIASA, Laxenburg, Austria and FAO, Rome, Italy: 2008.

Foster Stephen, Garduño Héctor, Kemper Karin. The 'COTAS': Progress with Stakeholder Participation in Groundwater Management in Guanajuato, Mexico. http://water.worldbank.org/sites/water.worldbank.org/files/GWMATE_CP10_Mexico2004_0.pdf.

GTO Secretaría De Desarrollo Agropecuario. Programa de Rehabilitación de Obras Hidroagrícolas del Agua Superficial.2012.

Gupta Hoshin Vijai, Sorooshian Soroosh, Yapo Patrice Ogou. Status of Automatic Calibration for Hydrologic Models: Comparison with Multilevel Expert Calibration [J]. Journal of Hydrologic Engineering, 1999, 4(2): 135-143.

Guzman-Soria Eugenio, Teresa De La Garza-Carranza Maria, Rebollar-Rebollar Samuel, et al. Econometric model for industrial and urban groundwater consumption in Guanajuato, Mexico: 1980-2011 [J]. Tecnología y Ciencias del Agua, 2013, 4(3): 187-193.

Hargreaves George H., Samani Zohrab A. Reference crop evapotranspiration from ambient air temperature. [J]. Applied Engineering in Agriculture, 1985, 1(2): 96-99.

Heo Joonghyeok, Yu Jaehyung, Giardino John R., et al. Water Resources Response to Climate and Land-Cover Changes in a Semi-Arid Watershed, New Mexico, USA [J]. Terrestrial, Atmospheric and Oceanic Sciences, 2015, 26(4): 463-474.

Herrera-Pantoja M., Hiscock K. M. Projected impacts of climate change on water availability indicators in a semi-arid region of central Mexico [J]. Environmental Science & Policy, 2015, 54: 81-89.

IPCC. Climate change 2007-impacts, adaptation and vulnerability: Working group II contribution to the fourth assessment report of the IPCC[M]. Cambridge University Press, 2007.

IPCC. Climate Change 2014: Synthesis Report. Contribution of Working Groups I, II and III to the Fifth Assessment Report of the Intergovernmental Panel on Climate Change. Geneva, Switzerland: 2014.

Jujnovsky J., Gonzalez-Martinez T. M., Cantoral-Uriza E. A., et al. Assessment of Water Supply as an Ecosystem Service in a Rural-Urban Watershed in Southwestern Mexico City [J]. Environmental Management, 2012, 49(3): 690-702.

Li Yanmei, Knappett Peter, Giardino John Rick, et al. The risk of supply of Surface/groundwater in the Laja River Basin in the State of Guanajuato, Mexico. Vienna, Austria: EGU General Assembly 2016, 2016.

Lopez-Morales Carlos A., Duchin Faye. Economic implications of policy restrictions on withdraws from surface and underground sources [J]. Economic Systems Research, 2015, 27(2): 154-171.

Magaña Víctor O., Vázquez Jorge L., Pérez José L., et al. Impact of El Niño on precipitation in Mexico [J]. GEOFISICA INTERNACIONAL-MEXICO-, 2003, 42(3): 313-330.

Mahlknecht J., Gárfias-Solis J., Aravena R., et al. Geochemical and isotopic investigations on groundwater residence time and flow in the Independence Basin, Mexico [J]. Journal of Hydrology, 2006, 324(1–4): 283-300.

Mahlknecht Jürgen. Estimation of recharge in the Independence aquifer, central Mexico, by combining geochemical and groundwater flow models [D]. Vienna, Austria: University of Agriculture and Life Sciences (BOKU)Institute of Applied Geology, 2003.

Mahlknecht Jürgen, Schneider Jean F., Merkel Broder J., et al. Groundwater recharge in a sedimentary basin in semi-arid Mexico [J]. Hydrogeology Journal, 2004, 12(5): 511-530.

Maier N., Dietrich J. Using SWAT for Strategic Planning of Basin Scale Irrigation Control Policies: a Case Study from a Humid Region in Northern Germany [J]. Water Resources Management, 2016, 30(9): 3285-3298.

Marek Gary W., Gowda Prasanna H., Evett Steven R., et al. Estimating Evapotranspiration for Dryland Cropping Systems in the Semiarid Texas High Plains Using SWAT [J]. JAWRA Journal of the American Water Resources Association, 2016, 52(2): 298-314.

Mateos Efrain, Santana Julio-Sergio, Montero-Martínez Martin J., et al. Possible climate change evidence in ten Mexican watersheds [J]. Physics and Chemistry of the Earth, Parts A/B/C, 2016, 91: 10-19.

Molina-Navarro Eugenio, Hallack-Alegría Michelle, Martínez-Pérez Silvia, et al. Hydrological modeling and climate change impacts in an agricultural semiarid region. Case study: Guadalupe River basin, Mexico [J]. Agricultural Water Management, 2016, 175(SI1): 29-42.

Moriasi D. N., Arnold J. G., Van Liew M. W., et al. Model evaluation guidelines for systematic quantification of accuracy in watershed simulations [J]. Transactions of the ASABE, 2007, 50(3): 885-900.

Mosbahi Manel, Benabdallah Sihem, Boussema Mohamed Rached. Sensitivity analysis of a GIS-based model: A case study of a large semi-arid catchment [J]. EARTH SCIENCE INFORMATICS, 2015, 8(3SI): 569-581.

Muñoz Piña Carlos, Sara Avila Forcada, Luis Armando Jaramillo Mosqueira, et al. Agriculture Demand for Groundwater in Mexico: Impact of water right enforcement and electricity user-fee on Groundwater level and quality.INE-SEMARNAT, 2006.

Nash J. E., Sutcliffe J. V. River flow forecasting through conceptual models part I — A discussion of principles [J]. Journal of Hydrology, 1970, 10(3): 282-290.

Navarro De León I., Gárfias-Soliz J., Mahlknecht J. Groundwater flow regime under natural conditions as inferred from past evidence and contemporary field observations in a semi-arid basin: Cuenca de la Independencia, Guanajuato, México [J]. Journal of Arid Environments, 2005, 63(4): 756-771.

Neitsch S. L., Arnold J. G., Kiniry J. R., et al. Soil & Water Assessment Tool: Theoretical Documentation, Version 2009, TR-406. College station, Texas: Texas Water Resource Institute, 2011.

NEX-GDDP. Advancing Research and Applications with NASA Climate Model Data. https://cds.nccs.nasa.gov/nex/.

Nie W., Yuan Y., Kepner W., et al. Hydrological impacts of mesquite encroachment in the upper San Pedro watershed [J]. Journal of Arid Environments, 2012, 82: 147-155.

NRC National Research Council. America's Climate Choices: Panel on Advancing the Science of Climate Change//Advancing the Science of Climate Change. Washington, D.C.: 2010.

OECD. OECD Environmental Performance Reviews: Mexico 2013.

Orozco-Ramírez Quetzalcóatl, Astier Marta. Socio-economic and environmental changes related to maize richness in Mexico’s central highlands [J]. Agriculture and Human Values, 2017, 34(2): 377-391.

Ortega-Guerrero M. A., Castellanos J. Z., Aguilar G R., et al. A conceptual model for increases of sodium, SAR, alkalinity and pH at the independence aquifer in Guanajuato [J]. Terra, 2002, 20(2): 199-207.

Ortega-Guerrero M. Adrián, Carrasco-Núñez Gerardo. Environmental occurrence, origin, physical and geochemical properties, and carcinogenic potential of erionite near San Miguel de Allende, Mexico [J]. Environmental Geochemistry and Health, 2014, 36(3): 517-529.

Pulido-Madrigal L., Simuta-Champo R., González-Meraz J., et al. Producción agrícola sustentable en condiciones de sobreexplotación de agua subterránea [J]. Terra Latinoamericana, 2012, 30(4): 303-313.

Riahi K., Grübler A., Nakicenovic N. Scenarios of long-term socio-economic and environmental development under climate stabilization [J]. Technological Forecasting and Social Change, 2007, 74(7): 887-935.

Rocha João, Roebeling Peter, Rial-Rivas María Ermitas. Assessing the impacts of sustainable agricultural practices for water quality improvements in the Vouga catchment (Portugal) using the SWAT model [J]. Science of The Total Environment, 2015, 536: 48-58.

Ropelewski Chester F., Halpert Michael S. North American precipitation and temperature patterns associated with the El Niño/Southern Oscillation (ENSO) [J]. Monthly Weather Review, 1986, 114(12): 2352-2362.

Sandoval Ricardo. A participatory approach to integrated aquifer management: The case of Guanajuato State, Mexico [J]. Hydrogeology Journal, 2004, 12(1): 6-13.

Saxton K. E., Rawls W. J. Soil water characteristic estimates by texture and organic matter for hydrologic solutions [J]. Soil science society of America Journal, 2006, 70(5): 1569-1578.

Seguí Oscar González. Estudios michoacanos Ⅹ [M]. El Colegio de Michoacán A.C., 2003.

Sheffield Justin, Wood Eric F., Munoz-Arriola Francisco. Long-term regional estimates of evapotranspiration for Mexico based on downscaled ISCCP data [J]. Journal of Hydrometeorology, 2010, 11(2): 253-275.

SMN Servicio Meteorológico Nacional. Información Climatológica por Estado. http://smn.cna.gob.mx/es/informacion-climatologica-ver-estado?estado=gto.

Solaymani Hamid R., Gosain A. K. Assessment of climate change impacts in a semi-arid watershed in Iran using regional climate models [J]. Journal of Water and Climate Change, 2015, 6(1): 161-180.

Torres-Benites E., Mejía-Sáenz E., Cortes-Becerra J., et al. Adaptation of a hydrological simulation model to the Rio Laja watershed, Guanajuato, Mexico [J]. Agrociencia, 2005, 39(5): 481-490.

UN-Water. Mexico - UN-Water Country Brief. http://www.unwater.org/fileadmin/user_upload/unwater_new/docs/Publications/MEX_pagebypage.pdf.

USGS. The World's Water. http://water.usgs.gov/edu/earthwherewater.html.

Wise M., Calvin K., Thomson A., et al. Implications of limiting CO2 concentrations for land use and energy [J]. Science, 2009, 324(5931): 1183-1186.

Wu Hongjing, Chen Bing. Evaluating uncertainty estimates in distributed hydrological modeling for the Wenjing River watershed in China by GLUE, SUFI-2, and ParaSol methods [J]. Ecological Engineering, 2015, 76: 110-121.

Zhang Ling, Nan Zhuotong, Xu Yi, et al. Hydrological Impacts of Land Use Change and Climate Variability in the Headwater Region of the Heihe River Basin, Northwest China [J]. PLOS ONE, 2016, 11(e01583946).